

Bone morphogenetic protein 4 (BMP4) alleviates hepatic steatosis by increasing hepatic lipid turnover and inhibiting the mTORC1 signaling axis in hepatocytes

Qi Peng^{1,*}, Bin Chen^{1,*}, Hao Wang^{1,2}, Ying Zhu¹, Jinghong Wu¹, Yetao Luo³, Guowei Zuo¹, Jinyong Luo¹, Lan Zhou¹, Qiong Shi¹, Yaguang Weng¹, Ailong Huang⁴, Tong-Chuan He², Jiaming Fan¹

¹Ministry of Education Key Laboratory of Diagnostic Medicine, and School of Laboratory Medicine, Chongqing Medical University, Chongqing 400016, China

²Molecular Oncology Laboratory, Department of Orthopaedic Surgery and Rehabilitation Medicine, The University of Chicago Medical Center, Chicago, IL 60637, USA

³Clinical Epidemiology and Biostatistics Department, Department of Pediatric Research Institute, Children's Hospital of Chongqing Medical University, Chongqing 400014, China

⁴Key Laboratory of Molecular Biology for Infectious Diseases of The Ministry of Education of China, Institute for Viral Hepatitis, Department of Infectious Diseases, The Second Affiliated Hospital of Chongqing Medical University, Chongqing, China

*Equal contribution

Correspondence to: Jiaming Fan; email: fanjiaming1988@cqmu.edu.cn

Keywords: non-alcoholic fatty liver disease (NAFLD), hepatic lipid metabolism, BMP signaling, mTORC1 signaling

Received: September 18, 2019 **Accepted:** November 19, 2019 **Published:** December 12, 2019

Correction: This article has been corrected. See Aging 2020 Jan. 13: <https://doi.org/10.18632/aging.102759>

Copyright: Peng et al. This is an open-access article distributed under the terms of the Creative Commons Attribution License (CC BY 3.0), which permits unrestricted use, distribution, and reproduction in any medium, provided the original author and source are credited.

ABSTRACT

Liver has numerous critical metabolic functions including lipid metabolism, which is usually dysregulated in obesity, the metabolic syndrome, and non-alcoholic fatty liver disease (NAFLD). Increasing evidence indicates bone morphogenetic proteins (BMPs) play an important role in adipogenesis and thermogenic balance in adipogenic progenitors and adipose tissue. However, the direct impact of BMPs on hepatic steatosis and possible association with NAFLD are poorly understood. Here, we found that BMP4 was up-regulated in oleic acid-induced steatosis and during the development of high fat diet (HFD)-induced NAFLD. Exogenous BMP4 reduced lipid accumulation and up-regulated the genes involved in lipid synthesis, storage and breakdown in hepatocytes. Exogenous BMP4 inhibited hepatic steatosis, reduced serum triglyceride levels and body weight, and alleviated progression of NAFLD *in vivo*. Mechanistically, BMP4 overexpression in hepatocytes down-regulated most components of the mTORC1 signaling axis. Collectively, these findings strongly suggest that BMP4 may play an essential role in regulating hepatic lipid metabolism and the molecular pathogenesis of NAFLD. Manipulating BMP4 and/or mTORC1 signaling axis may lead to the development of novel therapeutics for obesity, metabolic syndrome, and NAFLD.

INTRODUCTION

Liver is an essential organ in carrying out critical metabolic functions, ranging from metabolism of nutrients, synthesis of glucose and lipids, to detoxification of drugs and xenobiotics. Disruptions of

liver metabolic functions may lead to a broad range of liver diseases such as metabolic syndrome, obesity and cancer [1–4]. In fact, non-alcoholic fatty liver disease (NAFLD) resulted from obesity and the metabolic syndrome is the most common liver disease in the western world [1–4]. The pathological characteristics of

NAFLD is the accumulation of triglycerides (TG) within hepatocytes (also known as, hepatic steatosis) [1–4]. Hepatic lipid metabolism is tightly regulated by hormones (such as insulin), nuclear receptors, numerous cellular signaling pathways and transcription factors [1], although molecular mechanisms through which hepatic lipid metabolism are regulated remain to be fully understood.

Bone morphogenetic proteins (BMPs) belong to the TGF- β superfamily, and play important roles in regulating embryonic development, stem cell differentiation, and adult tissue homeostasis [5–9]. There are at least 14 types of BMPs in rodents and humans [6, 7, 10]. Through a comprehensive analysis of the 14 types of human BMPs, we have demonstrated that several osteogenic BMPs, such as BMP2, 4, 6, 7 and 9, are potent factors to drive adipogenic differentiation of mesenchymal stem cells [10–13]. We and others further showed that BMP7 and BMP4 may act as a molecular switch in regulating white vs. brown adipogenesis and energy expenditure [14–20]. Furthermore, BMP7 was shown to reverse obesity phenotype by regulating appetite through the central mTOR pathway in the brain [14]. However, the effect of BMPs on lipogenesis, metabolism and energy expenditure has been mostly investigated in adipogenic progenitors and adipose tissue. Thus, the direct impact of BMP signaling on hepatic metabolism, especially on glucose and lipid production, as well as possible association of BMP signaling with NAFLD, remains to be fully understood.

Here, we demonstrated that exogenous BMP4 inhibited the hepatic steatosis, lowered serum triglyceride (TG) and body weight, and alleviated the development and progression of NAFLD in a mouse model. We further demonstrated that BMP4 exerted the above effects by promoting lipid turnover through up-regulating the genes involved in lipid metabolism, while suppressing mTORC1 signaling pathway both *in vitro* and *in vivo*. These results strongly suggest that BMP4 may play an essential role in regulating hepatic lipid metabolism and should aid us to understand the molecular pathogenesis of NAFLD. It is conceivable that manipulating BMP4 and/or mTORC1 signaling networks would lead to the development of novel therapeutics for obesity, metabolic syndrome, and NAFLD.

RESULTS

BMP4 is up-regulated in Oleic acid-induced steatosis and during the development of a mouse model of NAFLD

Oleic acid can induce the triglyceride lipid accumulation significantly in cultured hepatocytes [21, 22]. We showed

that 0.05mm Oleic acid effectively induced hepatic triglyceride/lipid accumulation in 4-week-old mouse primary hepatocytes starting from days 3 to 7 contrast with that of control methanol group (Figure 1A, a). TqPCR assay and Western blotting analysis revealed that BMP4 expression was up-regulated upon oleic acid treatment of the primary hepatocytes (Figure 1A, b and c). We next examined the expression status of BMP4 in NAFLD. As shown in Figure 1B, we successfully established the mouse model of HFD-induced NAFLD as confirmed by H & E staining (Figure 1B, a) and ORO staining (Figure 1B, b) in the liver samples derived from the HFD group at weeks 16 and 24, compared with that of control group. Using Western blotting analysis, we found BMP4 expression in the liver samples was significantly up-regulated in the HFD group at week 16 and 24, compared with that of the control group (Figure 1C, a). Immunohistochemical staining further confirmed that BMP4 expression was elevated in the HFD group at weeks 16 and 24, compared with that of the control group (Figure 1C, b). Control IgG of liver tissue was shown in Supplementary Figure 1D, a. These results suggest that BMP4 expression may be associated with the development of hepatic steatosis.

Exogenous BMP4 inhibits triglyceride/lipid accumulation but plays a paradoxical role in regulating the expression of the genes involved in lipid metabolism in hepatocytes

To effectively deliver and overexpress of BMP4 into cultured hepatocytes and liver tissue *in vivo*, we constructed the recombinant adenovirus Ad-B4 and a mock control virus Ad-GFP. We demonstrated that Ad-B4 (and Ad-GFP) effectively infected primary hepatocytes and expresses a high level of BMP4 both at mRNA and protein levels (Supplementary Figure 1A and 1B). ORO staining showed that Ad-B4 significantly decreased hepatic triglyceride/lipid accumulation after 7 days, compared with that of Ad-GFP (Figure 2A). TqPCR results revealed that BMP4 up-regulated the expression of lipid synthesis and storage genes, such as *Gpam*, *Fasn*, *Srebf1* at 36h, and *Mogat*, *Acaca*, *Apoc3*, *Srebf1*, *Plin2*, *Lipe* at 72h (Figure 2B, a and b), as well as the expression of lipid breakdown genes, such as *Ascl2*, *Ndufs4*, *Cyp1a2*, *Acadm*, *Atp5a1*, *Hadha* at 36h, and *Ascl1*, *Ndufs4*, *Pck2*, *Cyp1a2*, *Acadm*, *Atp5a1*, *Hadha* at 72h (Figure 2B, c and d).

Exogenous BMP4 inhibits hepatic lipid accumulation via suppressing mTORC1 signaling pathway in hepatocytes

We next sought to delineate the mechanism underlying BMP4-inhibited hepatic steatosis. Using the PI3K/mTOR

inhibitor PF-04691502, we found both inhibitors effectively inhibited oleic acid-induced lipid accumulation in mouse primary hepatocytes (Figure 2C). BMP4 was shown to effectively inhibit the expression of mTORC1 signaling members, such as *S6k*, *Deptor*, *Pras40*, *Rptor*, *mTor*, and *Srebf1* at 36h and/or 72h after

Ad-B4 infection, while transiently up-regulating the expression of *Lipin1* at 36h after Ad-B4 infection (Figure 2D). Furthermore, through Western blotting analysis, we confirmed that BMP4 down-regulated the expression of DEPTOR, S6K, p-S6K and SREBF1, while up-regulating the expression of LIPIN1 at 72h (Figure 2E).

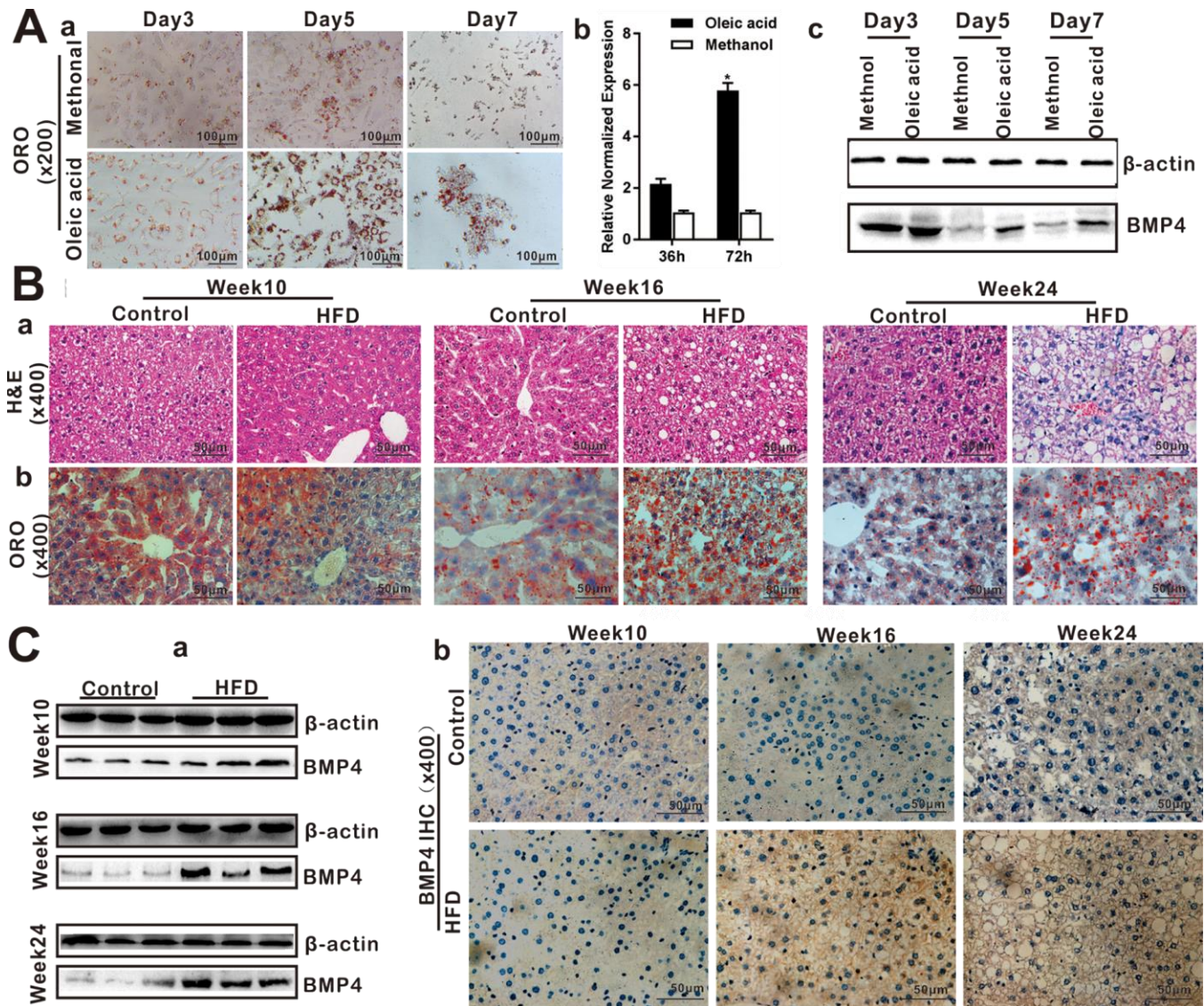


Figure 1. BMP4 expression is elevated during Oleic acid-induced triglyceride/lipid accumulation in hepatocytes and in a mouse model of NAFLD. (A) BMP4 expression in Oleic acid-induced lipid accumulation. Primary mouse hepatocytes were stimulated with 0.05mM Oleic acid (methanol as a vehicle control). ORO staining was done at days 3, 5 and 7 respectively. Representative images are shown (a). Alternatively, total RNA was isolated at 36h and 72h post Oleic acid treatment and subjected to TqPCR analysis of *Bmp4* expression. Relative expression was calculated by dividing the relative expression values (i.e., *Bmp4/Gapdh*) in “*” $p < 0.05$, Oleic acid group vs. methanol group (b). Total protein was isolated and subjected to Western blotting analysis of BMP4 expression at days 3, 5 and 7 post Oleic acid treatment (c). (B) Establishment of the mouse model of NAFLD. C57/B6 mice (4-week-old male, $n=10$ /time point/group) were fed with 45% high fat diet (HFD) or normal diet (Control), and sacrificed at weeks 10, 16 and 24, respectively. The retrieved liver tissue was subjected to H & E staining (a) and ORO staining (b). (C) BMP4 expression in mouse liver tissue of NAFLD. Total protein was isolated from the mouse liver tissue of the HFD and Control groups at weeks 10, 16 and 24 respectively, and subjected to Western blotting analysis of BMP4 expression. (a). IHC (immunohistochemical) staining of BMP4 expression was detected in the liver from the HFD and Control groups respectively (b). Each assay condition was done in triplicate, and representative images are shown or indicated by arrows.

Exogenous BMP4 suppresses hepatic triglyceride/lipid accumulation by up-regulating hepatic lipid turnover *in vivo*

To assess whether recombinant adenoviral vectors can mediate a sustained expression of transgenes via direct

intrahepatic injection, we injected CsCl gradient-purified Ad-FLuc and Ad-GFP control viruses via transdermal intrahepatic injection, followed by Xenogen optical imaging after injection. We found the FLuc signals were readily detected at least 5 days after injection (Supplementary Figure 1C). To minimize potential

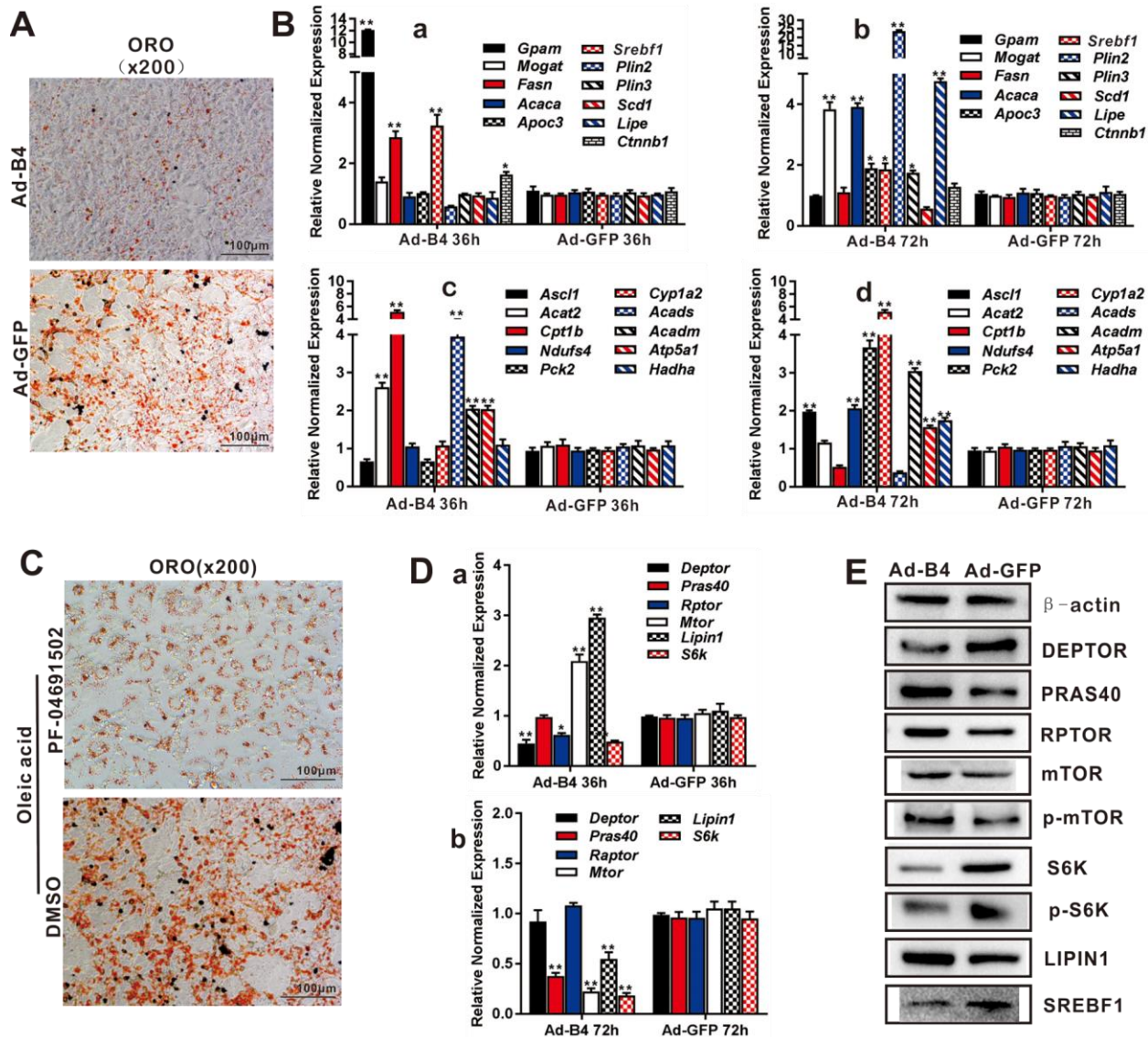


Figure 2. BMP4 inhibits triglyceride accumulation through regulating the genes involved in lipid metabolism and members of mTORC1 signaling pathway in hepatocytes. (A) Primary mouse hepatocytes were infected with Ad-B4 or Ad-GFP for 7 days, and subjected to ORO staining. (B) Primary mouse hepatocytes were infected with Ad-B4 or Ad-GFP for 36h and 72h. Total RNA was isolated and subjected to TqPCR analysis of the expression of the genes involved in triglyceride synthesis and storage (*a and b*) and triglyceride breakdown (*c and d*). Relative expression was calculated by dividing the relative expression values (i.e., gene/*Gapdh*) in “***” $p < 0.001$, “**” $p < 0.05$, Ad-B4 group vs. Ad-GFP group. (C) Oleic acid (0.05mM)-induced hepatocytes were treated with 1nM PF-04691502 or DMSO for 7 days, and subjected to ORO staining. (D) Primary mouse hepatocytes were infected with Ad-B4 or Ad-GFP for 36h and 72h. Total RNA was isolated and subjected to TqPCR analysis of the expression of the members of mTORC1 signaling pathway (*a and b*). Relative expression was calculated by dividing the relative expression values (i.e., gene/*Gapdh*) in “***” $p < 0.01$, “**” $p < 0.05$, Ad-B4 group vs. Ad-GFP group. (E) Primary mouse hepatocytes were infected with Ad-B4 or Ad-GFP for 72h, and total cell lysate was subjected to Western blotting analysis of the expression of the members of mTORC1 signaling pathway. Each assay condition was done in triplicate, and representative images are shown or indicated by arrows.

toxicities, the high titered Ad-B4 and Ad-GFP used for intrahepatic injections were purified through CsCl gradient ultracentrifugation as described [23, 24], and Ad-B4-mediated expression of BMP4 was further confirmed by Western blotting (Supplementary Figure 1B a and b).

We next tested the effect of exogenous BMP4 on hepatic lipid metabolism *in vivo*. Direct intrahepatic injections of Ad-B4 or Ad-GFP did not cause any apparent histologic changes in mouse liver after 4 weeks, while hepatocytes became swelling and some hepatic steatosis-like changes were observed in the Ad-GFP injection group, but not in the Ad-B4 injection group at 12 weeks, as assessed by H & E staining (Figure 3A, a). Furthermore, ORO staining revealed that Ad-B4 injection significantly inhibited hepatic lipid accumulation at both weeks 4 and 12 (Figure 3A, b). While no significant changes in the body weights and serum TG concentrations were observed at week 4 (Figure 3B, a and b), Ad-B4 injections led to the decreases in body weights and serum TG concentrations at week 12 (Figure 3B, c and d). Quantitative analysis using TqPCR further showed that exogenous expression of BMP4 significantly up-regulated the expression of lipid synthesis and storage genes (Figure 3C, a and c) and lipid breakdown genes (Figure 3C, b and d) at both weeks 4 and 12, suggesting BMP4 may promote the turnover rate of hepatic lipids *in vivo*.

Exogenous BMP4 blocks hepatic triglyceride/lipid accumulation and attenuates the development and progression of NAFLD *in vivo*

We further tested whether BMP4 could influence the disease process of NAFLD. When intrahepatic injections of Ad-B4 or Ad-GFP were initiated concurrently with the commencement of HFD-induced NAFLD in mice, hepatic steatosis-like changes were observed in the Ad-GFP injection group at 12-week time point, based on H & E staining while we did not observe any apparent histologic changes of the liver in both Ad-B4 and Ad-GFP groups at 4-week time point (Figure 4A, a). ORO staining revealed that Ad-B4 injection significantly suppressed lipid accumulation in the liver, compared with that of the Ad-GFP injection group, at both 4-week and 12-week time points (Figure 4A, b). Body weight measurements indicated that Ad-B4 injection significantly decreased the body weights at week 12 (Figure 4B, a and b), and there was a detectable decrease in serum TG levels in the Ad-B4 injection group at week 12 as well (Figure 4B, c and d). Furthermore, TqPCR analysis revealed that BMP4 injections effectively affected the expression of lipid synthesis and storage genes (Figure 4C, a and c) and lipid breakdown genes (Figure 4C, b and d) at both weeks 4 and 12, suggesting

that exogenous BMP4 may significantly impact the dysregulated lipid metabolism during the development of NAFLD.

Exogenous BMP4 inhibits hepatic steatosis and the development/progression of NAFLD by suppressing the mTORC1 signaling pathway *in vivo*

We explored the underlying mechanism of BMP4 action and analyzed the expression of mTOR signaling components in the liver samples isolated from the normal mice injected with Ad-B4 or Ad-GFP. Using Western blotting analysis, we found that intrahepatic injection of Ad-BMP4 decreased the expression of DEPTOR, PRAS40, S6K, p-S6K and SREBF1, and up-regulated the expression of RPTOR, p-mTOR, LIPIN1 at week 4 (Figure 5A). Similarly, BMP4 injections decreased the expression of DEPTOR, p-mTOR, S6K, p-S6K and SREBF1 and up-regulated the expression of the PRAS40, RPTOR, LIPIN1 at week 12 (Figure 5A). Furthermore, immunohistochemical staining showed that S6K and p-S6K significantly were down-regulated while LIPIN1 was up-regulated with increased nucleus staining by BMP4 both at weeks 4 and 12 (Figure 5B). Control IgG of liver tissue was shown in Supplementary Figure 1D, b.

Lastly, we examined the effect of exogenous BMP4 on mTOR signaling in NAFLD. Western blotting analysis revealed that Ad-B4 injections decreased the expression of S6K, p-S6K and SREBF1, while increased the expression of LIPIN1 both at weeks 4 and 12 (Figure 6A). Furthermore, immunohistochemical staining showed that Ad-B4 injections significantly down-regulated S6K, p-S6K and SREBF1 while increasing LIPIN1 expression in nucleus both at weeks 4 and 12 (Figure 6B). Control IgG of liver tissue was shown in Supplementary Figure 1D, c.

Collectively, these results strongly suggest that exogenous BMP4 may suppress hepatic steatosis and alleviate the development and progression of NAFLD by inhibiting mTORC1 signaling (Figure 7).

DISCUSSION

In this study, we investigated the direct effect of BMPs on hepatic metabolism and their potential links with NAFLD. We found that BMP4 expression was elevated during the development of mouse model of NAFLD, whereas exogenous BMP4 was shown to inhibit hepatic triglyceride/lipid accumulation by promoting lipid turnover and by suppressing the mTORC1 signaling pathway. These results also suggest that the elevated BMP4 expression in NAFLD may be caused by a feedback inhibition mechanism.

BMPs, mostly BMP2, BMP4 and BMP7, have been shown to play important roles in regulating adipogenesis, thermogenesis, and energy metabolism in adipocyte progenitor cells and adipose tissue, and/or at whole

animal levels [14–20]. An early study revealed that BMP2 induced a phenotypic change of C3H10T1/2 stem cells from the parental fibroblast to adipocytes and osteoblasts [25], while TGF- β and activin A were shown

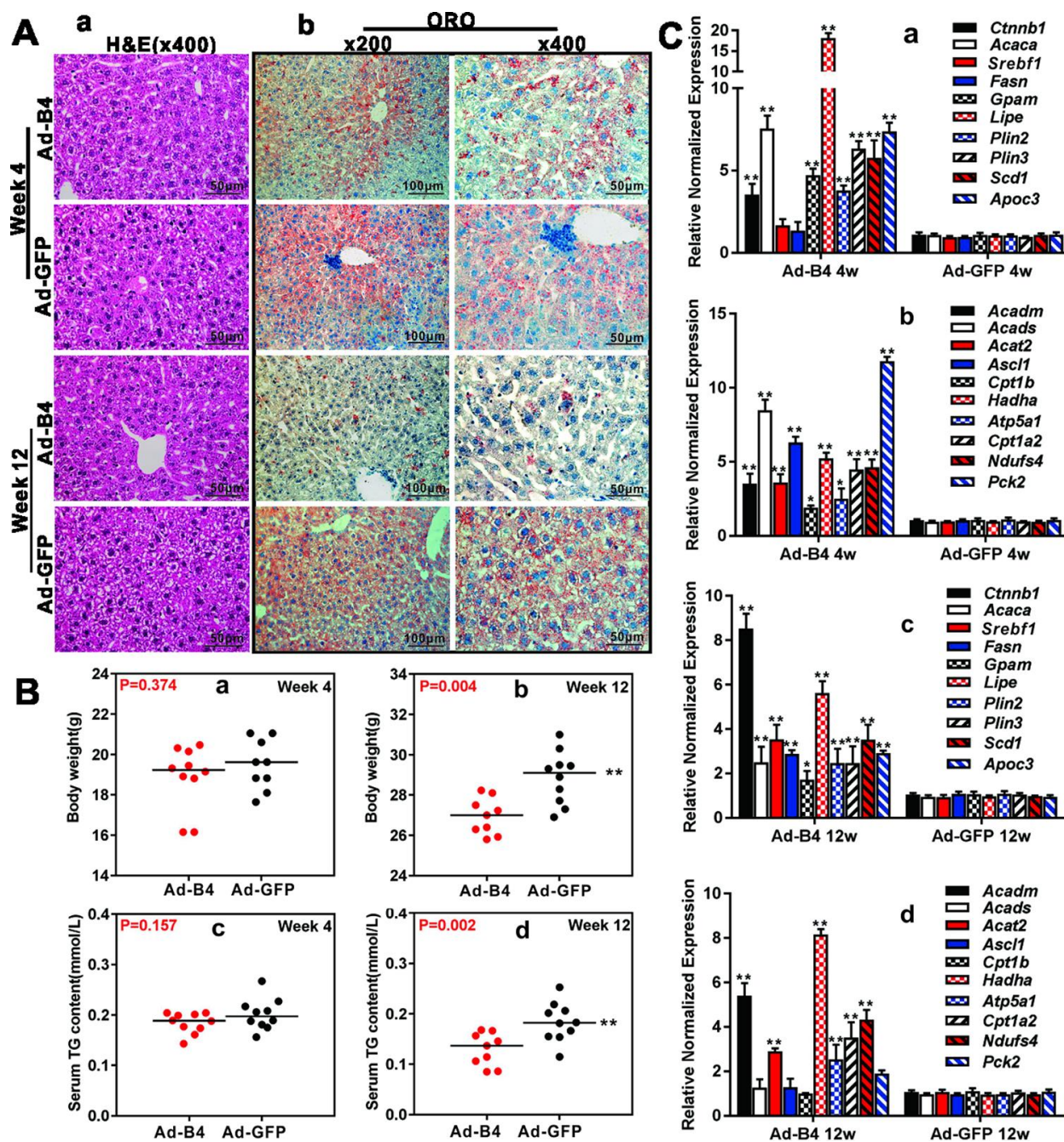


Figure 3. Exogenous BMP4 decreases the body weights, inhibits serum and hepatic triglyceride accumulation *in vivo*. (A) Ad-B4 or Ad-GFP was intrahepatically injected into 4-week old mice. The mice were sacrificed at weeks 4 and 12, and the retrieved liver tissue was subjected to H & E staining (a) and ORO staining (b). (B) The mouse body weights at weeks 4 and 12 (a and b), and serum total triglyceride (TG) (c and d) at weeks 4 and 12 were measured respectively. (C) Total RNA was isolated from the liver tissue of the mice injected with Ad-B4 or Ad-GFP at weeks 4 and 12 respectively, and TqPCR analysis was carried out to detect the expression of triglyceride synthesis and storage related genes (a and c) and triglyceride breakdown related genes (b and d). All samples were normalized with *Gapdh*. Relative expression was calculated by dividing the relative expression values (i.e., *gene/Gapdh*) in “***” $p < 0.01$, “**” $p < 0.05$, Ad-B4 group vs. Ad-GFP group. Each assay condition was done in triplicate, and representative images are shown or indicated by arrows.

to inhibit adipocyte development [26]. BMP4 was shown to drive pluripotent C3H10T1/2 stem cells to adipocyte lineage [27], which requires functional BMP/Smad signaling pathway [28].

Forced expression of BMP4 in white adipocytes reduced the mass of white adipocyte tissue (WAT) and the size of white adipocytes in mice, with an increased number of a white adipocyte cell types

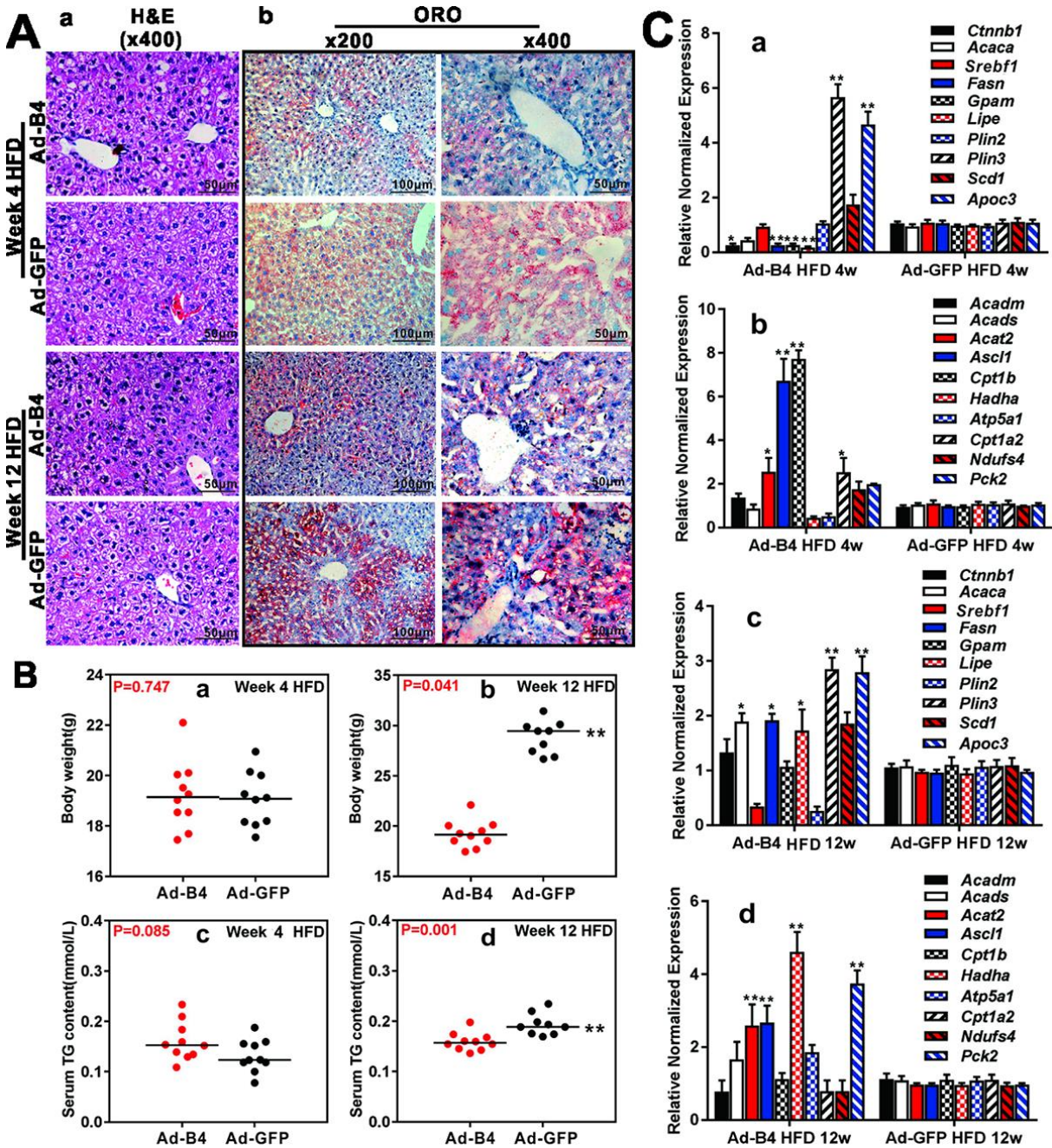


Figure 4. Exogenous BMP4 alleviates lipid accumulation and inhibits the development and progression of a mouse model of NAFLD. Ad-B4 or Ad-GFP were intrahepatically injected into the mice treated with HFD, and the mice were sacrificed at weeks 4 and 12 for following analyses. (A) The retrieved liver tissue was subjected to H & E staining (a) and ORO staining (b). (B) The body weights at weeks 4 and 12 (a and b), and serum total triglyceride (TG) at weeks 4 and 12 (c and d) were measured respectively. (C) Total RNA was isolated from the retrieved liver tissue of the HFD mice injected with Ad-B4 or Ad-GFP at weeks 4 and 12 respectively, and subjected to TqPCR analysis of the expression of triglyceride synthesis and storage related genes (a and c) and triglyceride breakdown related genes (b and d). All samples were normalized with *Gapdh*. Relative expression was calculated by dividing the relative expression values (i.e., *gene/Gapdh*) in “***” $p < 0.01$, “**” $p < 0.05$, Ad-B4 group vs. Ad-GFP group. Each assay condition was done in triplicate, and representative images are shown.

with brown adipocyte characteristics [16], which closely correlated with increased energy expenditure, improved insulin sensitivity, and protection against diet-induced obesity and diabetes [16]. Furthermore, silencing the BMP antagonist GREM1 and/or adding BMP4 during white adipogenic differentiation were shown to reactivate

beige/brown markers [29]. It was shown that selective brown adipose tissue overexpression of *Bmp4* in mice induced a shift from a brown to a white-like adipocyte phenotype [17], suggesting that *Bmp4* may be an important factor in the context of obesity and type 2 diabetes. Similarly, increased circulating BMP4 in

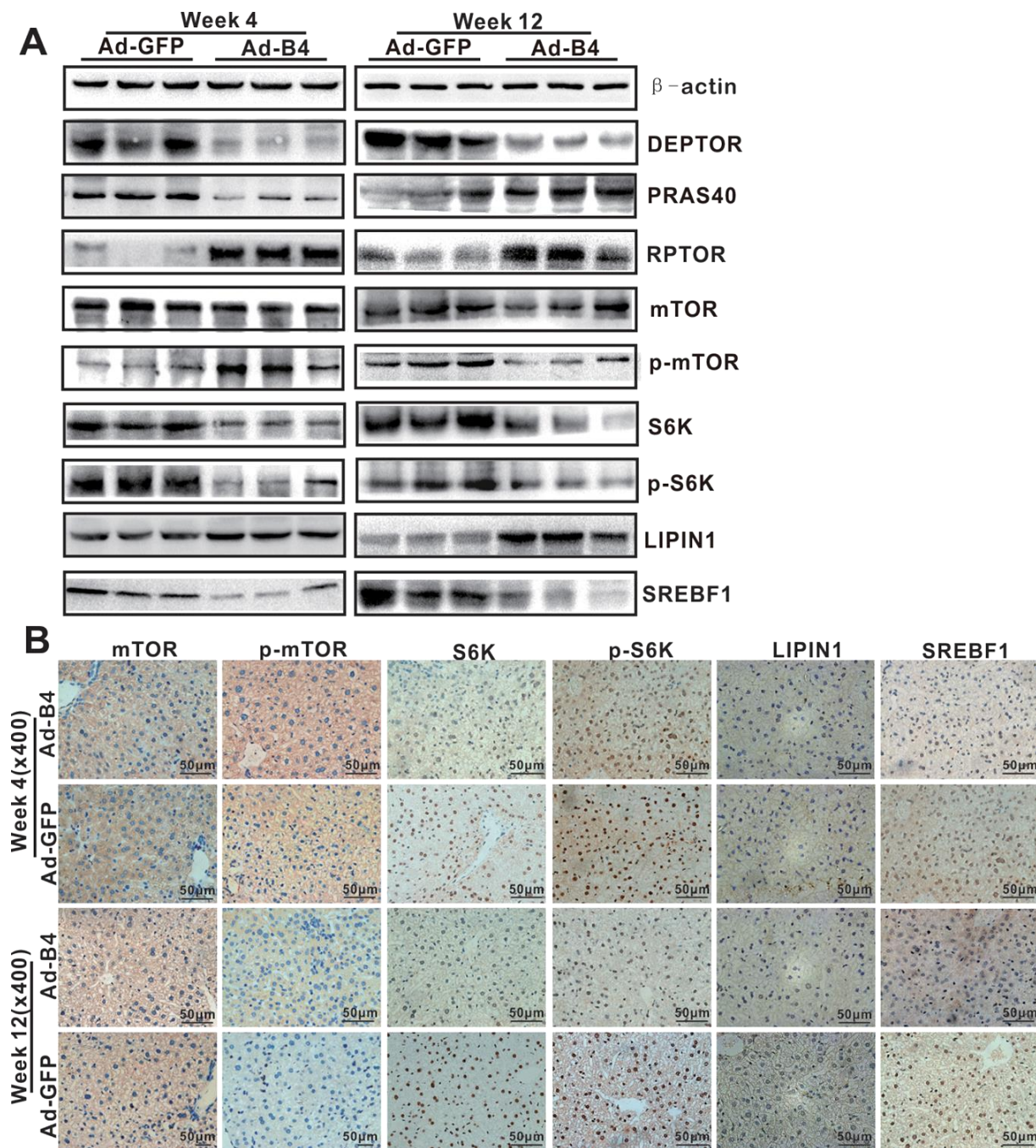


Figure 5. BMP4 down-regulates the mTORC1 signaling pathway in mouse liver. The liver samples prepared in Figure 3 were used for the following assays. (A) Total cell lysate was prepared from the retrieved liver samples and subjected to Western blotting analysis of the expression of the members of mTORC1 signaling pathway. (B) The retrieved liver samples were paraffin-embedded, sectioned and subjected to IHC staining to detect the expression of the members of mTORC1 signaling pathway and lipid metabolism. Each assay condition was done in triplicate, and representative images are shown.

mature mice prevented obesity and insulin resistance, and promoted subcutaneous WAT browning, leading to increased energy expenditure [19].

Nonetheless, it remains to be fully determined whether BMP-regulated lipid metabolism affects the development

and/or progression of obesity, metabolic syndrome and NAFLD. A small cohort study showed that serum BMP4 levels were significantly increased in individuals with obesity or metabolic syndrome [30]. Several BMPs and BMP receptors were implicated in obesity-related traits in humans [26]. Genetic variants of BMP receptor 1A

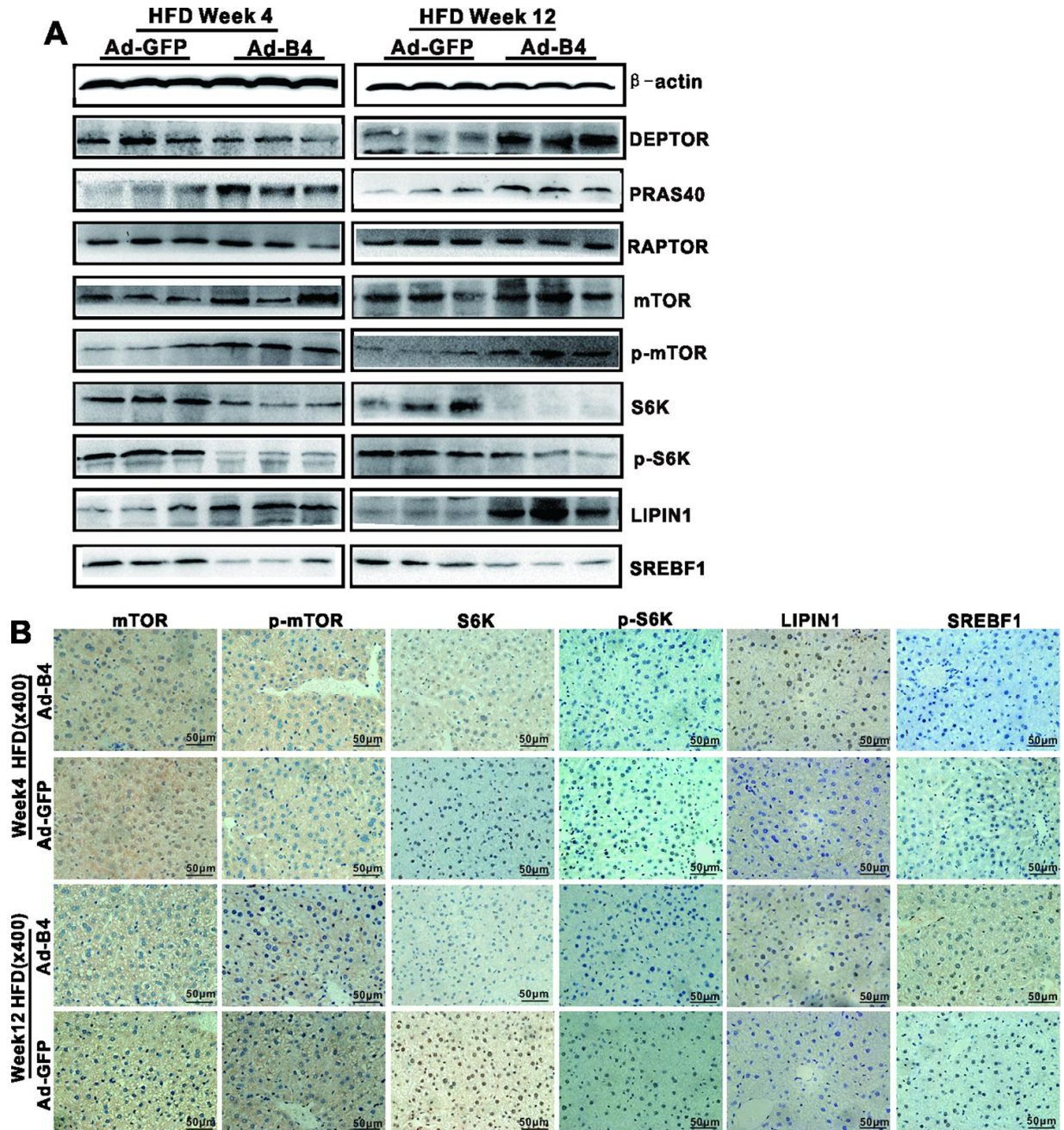


Figure 6. Exogenous BMP4 attenuates the development and progression of NAFLD by suppressing the mTORC1 signaling pathway. The liver samples prepared in Figure 4 were used for the following assays. (A) Total cell lysate prepared from the retrieved liver samples was subjected to Western blotting analysis to detect the expression of the members of mTORC1 signaling pathway and lipid metabolism. (B) The retrieved liver samples were paraffin-embedded, sectioned and subjected to IHC staining to detect the expression of the members of mTORC1 signaling pathway and lipid metabolism. Each assay condition was done in triplicate, and representative images are shown

gene (BMPRI1A) were associated with human obesity [31]. As essential for BMP signaling BMP receptor 2 (BMPRII) was implicated in adipogenesis and pathophysiology of obesity [32]. Interestingly, intracerebroventricular administration of BMP7 was shown to ameliorate the HFD-associated metabolic complications, suggesting that BMP7 may be explored as an attractive obesity therapeutic for diet-induced obesity and leptin-resistant conditions [14]. Rapamycin (mTOR), a kinase that is activated by anabolic signals, plays fundamental roles in regulating lipid biosynthesis and metabolism. The mTOR kinase nucleates two large protein complexes named mTOR complex 1 (mTORC1) and mTOR complex 2 (mTORC2) [35]. Both mTORC1 and mTORC2 share four protein components, including the TOR kinase, DEP domain-containing mTOR-interacting protein (DEPTOR) and mammalian lethal with Sec13 protein 8 (mLST8), while regulatory-associated protein of mTOR (RAPTOR) and proline-rich AKT substrate 40 kDa (PRAS40) are specific to mTORC1 [35, 36]. mTORC1 promotes protein synthesis and lipid synthesis,

which rely on the phosphorylation of mTORC1 substrates, including ribosomal S6 kinase 1 (S6K1), eukaryotic translation initiation factor 4E (eIF4E)-binding proteins 1 and 2 (4E-BP1/2), UNC-5 like autophagy activating kinase (ULK1), and transcription factor EB (TFEB) [35, 37]. Hepatic Lipogenesis is catalyzed by the rate-limiting enzymes acetyl-CoA carboxylase (ACC) and fatty acid synthase (FAS), both of which are transcriptionally controlled by various transcriptional regulators in response to nutrients and hormones, including sterol response element-binding protein (SREBP) family members, carbohydrate-responsive element binding protein (ChREBP), and nuclear receptors (PPAR γ , FXR, and LXR) [38, 39]. mTORC1 enhances lipogenesis via the positive regulation of SREBPs in an S6K1-dependent and S6K1-independent manner [40]. SREBPs belong to the family of basic helix-loop-helix-leucine zipper (bHLH-Zip) transcription factors, among which SREBP1c and SREBP2 are the major isoforms expressed in the liver [41]. The mechanism of S6K1-dependent

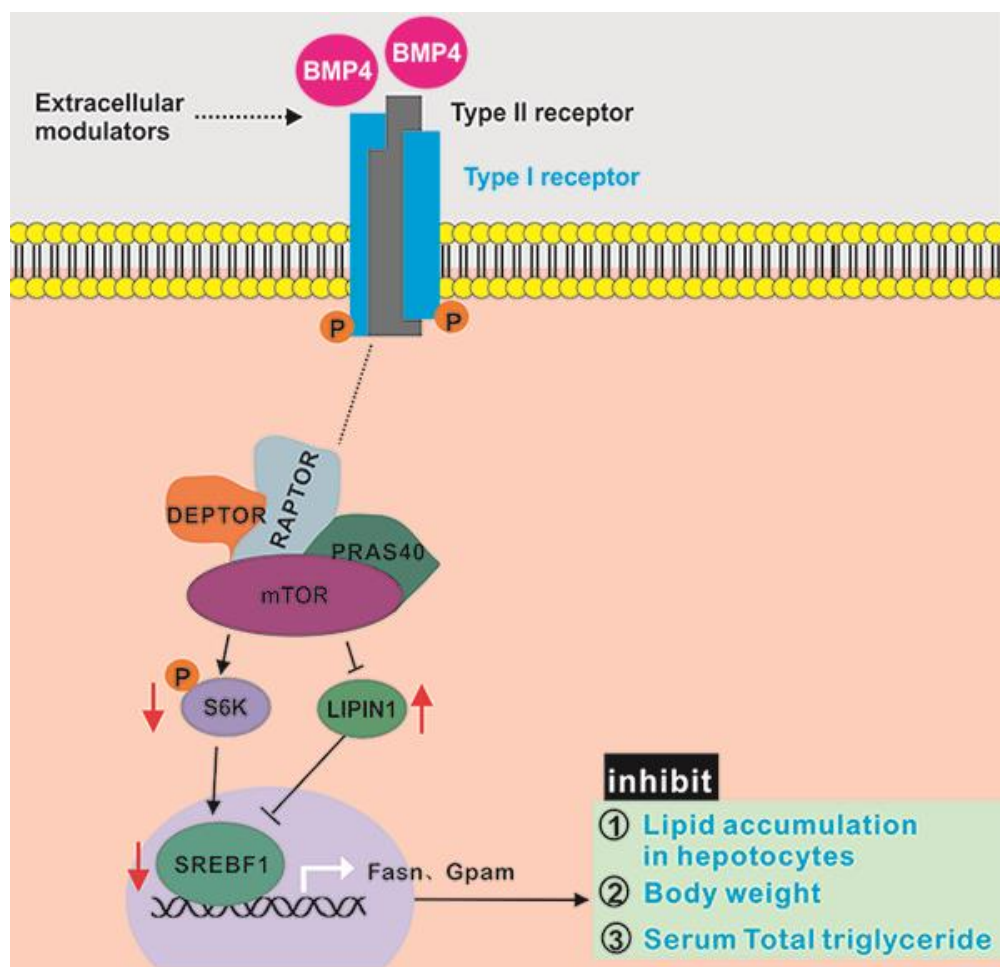


Figure 7. BMP4 may suppress hepatic steatosis and alleviate the development and progression of NAFLD by inhibiting mTORC1 signaling. BMP4 decrease the expression of S6K, p-S6K and SREBF1, while increase the expression of LIPIN1.

activation of SREBP is unclear, while the S6K1-independent activation of SREBP involves inhibition and phosphorylation of CRTC2 (CREB regulated transcription coactivator 2) and Lipin-1 (a phosphatidic acid phosphatase required for glycerolipid biosynthesis) [41–43]. Our studies may provide a possible mechanistic link between BMP signaling and mTOR pathway in lipid metabolism. In summary, we demonstrated that exogenous BMP4 inhibited the hepatic steatosis and alleviated the development and progression of NAFLD in a mouse model. Mechanistically, BMP4 exerted these effects by promoting lipid turnover through up-regulating the genes involved in lipid metabolism, while suppressing mTORC1 signaling pathway. Thus, our findings strongly suggest that BMP4 may play an essential role in regulating hepatic lipid metabolism and the molecular pathogenesis of NAFLD. It is conceivable that manipulating BMP4 and/or mTORC1 signaling networks would lead to the development of novel therapeutics for obesity, metabolic syndrome, and NAFLD.

MATERIALS AND METHODS

Cell culture and chemicals

293pTP and RAPA cells were derived from HEK-293 cells as previously described [44, 45]. Primary hepatocyte were prepared from 4-week-old C57BL/6J mice (both genders) using the type I collagenase/liver perfusion protocol as described [46]. All above cells were maintained in complete DMEM supplemented with 10% fetal bovine serum (Lonsa Science SRL), 100 units of penicillin and 100 mg of streptomycin at 37°C in 5% CO₂. Unless indicated otherwise, all chemicals were purchased from Sigma-Aldrich (St Louis, MO, USA), Thermo Fisher Scientific (Waltham, MA, USA), and/or Solarbio (Beijing, China).

Construction, amplification and purification of recombinant adenoviruses

Recombinant adenoviruses Ad-B4 and Ad-FLuc were constructed by using the AdEasy technology [23, 47]. Briefly, the full-length coding regions of human BMP4 and firefly luciferase were PCR amplified and subcloned into an adenoviral shuttle vector, pAdTrack-CMV. The resultant vectors were used to generate recombinant adenoviral vectors, pAd-B4 and pAd-FLuc, through homologous recombination with an adenoviral backbone vector in bacterial BJ5183 cells, which were subsequently used to generate recombinant adenoviruses Ad-B4 and Ad-FLuc in 293pTP or RAPA cells. The resulting adenoviruses Ad-B4 and Ad-FLuc also co-express GFP as a marker for tracking infection efficiency as described [11, 48]. An analogous adenovirus

expressing GFP only, Ad-GFP, was used as a mock control [49–51]. Polybrene (final concentration at 8 µg/ml) was added to enhance adenoviral infection efficiency [52]. For the direct *in vivo* injection studies, the adenoviruses (Ad-B4, Ad-FLuc and Ad-GFP) were purified through CsCl gradient ultracentrifugation, followed by desalting dialysis immediately prior to use, as described [23, 53].

Oil Red O (ORO) staining for triglyceride/lipid accumulation

ORO staining was carried out as described [11, 54]. Briefly, primary mouse hepatocyte was seeded in 24-well culture plates and treated with different conditions for 10 days. Alternatively, frozen sections from freshly prepared liver tissue samples were washed with PBS twice to remove embedding agents at room temperature (RT). Both cells and frozen sections were then fixed with 4% paraformaldehyde for 10 min at RT, briefly incubated in 60% isopropanol, and then stained with freshly-prepared ORO solution for 15 min at RT, followed by multiple washes with PBS as described [11, 54]. The staining results were recorded under a bright field microscope (magnification, x200 for cells and x400 for tissue). Each assay condition was done in triplicate.

Total RNA isolation of tissues/cells and touchdown-quantitative real-time PCR (TqPCR) analysis

Total RNA was isolated from both cells and freshly-prepared liver tissues by using the TRIZOL Reagent (Invitrogen, China) as described [55, 56]. Briefly, fresh mouse liver samples at different development stages (n=5, CD1 male, each time point) or from the NAFLD model were dissected out, minced, and ground in TRIzol Reagent. Similarly, primary mouse hepatocytes were treated with different conditions and lysed in TRIzol Reagent for total RNA isolation. Total RNA was subjected to reverse transcription with hexamer and M-MuLV reverse transcriptase (New England Biolabs, Ipswich, MA). The cDNA products were used as qPCR templates. The gene-specific PCR primers were designed by using Primer3 Plus (Supplementary Table 1). TqPCR was carried out by using 2x SYBR Green qPCR Master Mix (Bimake, Shanghai, China) on a CFX-Connect unit (Bio-Rad Laboratories, Hercules, CA) as described [57, 58]. All TqPCR reactions were done in triplicate. *Gapdh* was used as the reference gene. Quantification of gene expression was carried out by using the 2^{-ΔΔCq} method as described [59].

Western blotting analysis

Western blotting assay was carried out as described [60, 61]. Briefly, subconfluent primary hepatocytes were

infected with Ad-B4 and Ad-GFP for 72h. Cell lysates were prepared and subjected to SDS-PAGE, followed by electro-transferring to PVDF membranes, which were blocked and incubated overnight with the primary antibodies against β -ACTIN (1:5000-1:20000 dilution; Proteintech; Cat#60008-1-Ig), BMP4 (1:1000-1:3000 dilution; GeneTex; Cat#GTX100874), DEPTOR(1:100 dilution; Santa Cruz Biotechnology; Cat#sc-398169), PRAS40 (1:100 dilution; Santa Cruz Biotechnology; Cat#sc-517355), RPTOR (1:100 dilution; Santa Cruz Biotechnology; Cat#sc-81537), MTOR (1:1000-1:3000 dilution; GeneTex; Cat#GTX101557), p-MTOR (phospho Ser2448 1:1000-1:3000 dilution; GeneTex; Cat#GTX132803), S6K (1:1000-1:3000 dilution; GeneTex; Cat#GTX107562), p-S6K(phosphor S424 1:1000-1:3000 dilution; Abcam; Cat#ab131436), LIPIN1 (1:1000-1:3000 dilution; Abcam; Cat#ab181389) and SREBF1 (1:1000-1:3000 dilution; Proteintech; Cat#14099-1-AP). After being washed, the membranes were incubated with respective secondary antibodies (1:5000 dilution; ZSGB-BIG; Peroxidase-Conjugated Rabbit anti-Goat IgG or Peroxidase-Conjugated Goat anti-Mouse IgG; Cat#ZB-2306 or 2305). Immune-reactive signals were visualized by using the Enhanced Chemiluminescence (ECL) kit (Millipore, USA) on the Bio-Rad ChemiDoc Imager (Hercules, CA).

Measurement of serum triglyceride (TG) in mice

At each endpoint, the animals were anesthetized and subjected to cardiac puncture to collect whole blood as described [62], followed by centrifugation at 800 x g, 10min, RT. The collected sera were used to determine triglyceride (TG) concentrations by using the Triglyceride Assay kit in microplate reader format (Single reagent GPO-PAP; Nanjing Jiancheng Bioengineering Institute, China).

Establishment of the mouse model of non-alcoholic fatty liver disease (NAFLD)

The use and care of animals in the present study was approved by the Ethics Committee for Research and Experimental Animal Use of Chongqing Medical University (Chongqing, China; Certificate No: SCXK (YU)20070001). All animal experiments were performed in accordance with US National Institutes of Health Guide for the Care and Use of Laboratory animals [63]. The NAFLD model was established as described [64]. Briefly, 60 C57BL/6 (male, 4-week-old) were obtained from and housed at the Chongqing Medical University Experimental Animal Research Center. The mice were randomly divided into two groups (n=30 each): a high-fat diet (HFD) group fed with 45% fat diet (Medicience, Yangzhou, China) and a control group fed with 10% fat diet (Supplementary

Table 2). Ten mice from each group were sacrificed at weeks 10, 16 and 24, respectively. The retrieved liver tissue samples were either fixed with 4% paraformaldehyde for histologic and immunohistochemical analyses, or snap-frozen in liquid nitrogen for total RNA/protein isolation.

H & E staining and immunohistochemical (IHC) staining

The retrieved mouse liver samples were fixed in 4% paraformaldehyde overnight, paraffin embedded, and sectioned. The sections were deparaffinized, rehydrated and subjected to H & E staining and IHC staining as described [50, 58, 65, 66]. Briefly, the sections were subjected to deparaffinization, followed by H & E. For IHC staining, the sections were subjected to deparaffinization, followed by antigen retrieval and immunostaining with antibodies against BMP4 (1:100-1:200 dilution; GeneTex; Cat#GTX100874), mTOR (1:100-1:200 dilution; GeneTex; Cat#GTX101557), p-mTOR (phospho Ser2448 1:100-1:200 dilution; GeneTex; Cat#GTX132803), S6K (1:100-1:200 dilution; GeneTex; Cat#GTX107562), p-S6K (phosphor S424 1:100-1:200 dilution; Abcam; Cat#ab131436), LIPIN1 (1:100-1:200 dilution; Abcam; Cat#ab181389), and SREBP1 (1:100-1:200 dilution; Proteintech; Cat#14099-1-AP). Control rabbit IgG was used as a negative control (1:200 dilution; Abcam; Cat#ab97051).

Optical bioluminescence imaging of the mice with intrahepatic injection of Ad-FLuc

The *in vivo* use of recombinant adenoviruses was approved by the Ethics Committee for Research and Experimental Animal Use of Chongqing Medical University. To assess the duration of adenovirus-mediated gene expression in liver, we injected the CsCl gradient purified Ad-FLuc into mouse liver (4-week-old male, 10^{10} pfu/injection/mouse). Whole body optical imaging was performed at day 5 after injection by using D-Luciferin Potassium (Gold Biotechnology Inc.) as luciferase substrate and assessed with the Xenogen IVIS 200 Imaging System as described [67–70].

Intrahepatic delivery of Ad-B4/Ad-GFP into mice

The *in vivo* use of recombinant adenoviruses was approved by the Ethics Committee for Research and Experimental Animal Use of Chongqing Medical University. Animals were obtained from and housed in the Chongqing Medical University Experimental Animal Research Center, and the experimental procedure was carried out as previously described [71]. Briefly, 40 male 4-week-old C57BL/6 mice were randomly divided into two groups (n=20 each) with normal diet fed: an Ad-B4

group (i.e., Ad-B4), and an Ad-GFP group (i.e., Ad-GFP). 40 male interpretation period C57BL/6 mice were randomly divided into two groups (n=20 each) with high fat diet (HFD) fed: a HFD treated with Ad-BMP4 group (i.e., Ad-B4 HFD), and a HFD fed with Ad-GFP group (i.e., Ad-GFP HFD). Intrahepatic injections of Ad-B4 or Ad-GFP (10^{10} pfu in 30 μ l PBS/injection/animal) were initiated immediately after the mice were fed with normal diet or HFD, and were re-dosed every 5 days, based on optical imaging of the Ad-FLuc intrahepatic injection in C57BL/6 mice. Ten mice from each group were sacrificed at weeks 4 and 12, respectively. The retrieved liver tissue was either fixed with 4% paraformaldehyde or snap-frozen in liquid nitrogen for total RNA/protein isolation.

Statistical analysis

All quantitative experiments were performed in triplicate and/or repeated three times. Data were expressed as mean \pm standard deviation (SD). The Least Significant Difference (LSD) was performed following the one-way analysis of variance (ANOVA) analysis to determine significant differences between groups. A value of $p < 0.05$ was considered statistically significant.

Abbreviations

NAFLD: non-alcoholic fatty liver disease; Bmp4: bone morphogenetic protein 4; Ad-B4: Adenovirus-overexpression of BMP4; Ad-GFP: Adenovirus-expression of Green fluorescent protein (GFP); TG: triglycerides; ORO: Oil red O; TqPCR: touchdown-quantitative real-time PCR; IHC: immunohistochemical; H&E: hematoxylin and eosin; TG: triglycerides; Gpat: glycerol-3-phosphate acyltransferase, mitochondrial; Mogat1: monoacylglycerol O-acyltransferase 1; Fasn: fatty acid synthase; Acaca: acetyl-CoA carboxylase alpha; Apoc3: apolipoprotein C3; Srebf1/Srebp: sterol regulatory element binding transcription factor 1; Plin2: perilipin 2; Plin3: perilipin 3; Scd1: stearoyl-Coenzyme A desaturase 1; Lipe: lipase E, hormone sensitive type; Ctnnb1: catenin beta 1; Ascl1: achaete-scute family bHLH transcription factor 1; Acat2: acetyl-CoA acetyltransferase 2; Cpt1b: carnitine palmitoyltransferase 1B; Ndufs4: NADH: ubiquinone oxidoreductase subunit S4; Pck2: phosphoenolpyruvate carboxykinase 2, mitochondrial; Cyp1a2: cytochrome P450 family 1 subfamily A member 2; Acads(Bcd-1): acyl-CoA dehydrogenase short chain; Acadm: acyl-CoA dehydrogenase medium chain; Atp5a1: ATP synthase, H⁺ transporting, mitochondrial F1 complex, alpha subunit 1; Hadha: hydroxyacyl-CoA dehydrogenase trifunctional multienzyme complex subunit alpha; Deptor: DEP domain containing MTOR interacting protein; Pras40/Akt1s1: AKT1 substrate 1 (proline-rich); Rptor: regulatory associated protein of MTOR, complex 1;

Mtor: mechanistic target of rapamycin kinase; Rps6kb1/S6k: ribosomal protein S6 kinase B1.

AUTHOR CONTRIBUTIONS

JMF, TCH, and AH: Conceived the project and oversaw the study; QP, BC and HW: Performed most of the in vitro and in vivo experiments, and collected data; YZ and JW: performed H & E and IHC analyses; GZ, JL, LZ, QS and YW: provided essential experimental supports and important research resources; YL and JMF: data analysis and statistical analysis; JMF and TCH: drafted the manuscript; All authors: reviewed and approved the manuscript.

CONFLICTS OF INTEREST

The authors declare that the authors have no competing interests.

FUNDING

The reported study was supported in part by research grants from the 2017 Chongqing Postdoctoral Innovation Talent Support Program (JMF) and the 64th China Postdoctoral Science Fund (JMF), the National Key Research and Development Program of China (2016YFC1000803), 2019 Chongqing Municipal Education Commission Science and Technology Research Project (KJQN201900410). TCH was also supported by the Mabel Green Myers Research Endowment Fund and The University of Chicago Orthopaedic Surgery Alumni Fund.

REFERENCES

1. Bechmann LP, Hannivoort RA, Gerken G, Hotamisligil GS, Trauner M, Canbay A. The interaction of hepatic lipid and glucose metabolism in liver diseases. *J Hepatol.* 2012; 56:952–64. <https://doi.org/10.1016/j.jhep.2011.08.025> PMID:22173168
2. Michelotti GA, Machado MV, Diehl AM. NAFLD, NASH and liver cancer. *Nat Rev Gastroenterol Hepatol.* 2013; 10:656–65. <https://doi.org/10.1038/nrgastro.2013.183> PMID:24080776
3. Petersen MC, Vatner DF, Shulman GI. Regulation of hepatic glucose metabolism in health and disease. *Nat Rev Endocrinol.* 2017; 13:572–87. <https://doi.org/10.1038/nrendo.2017.80> PMID:28731034
4. Samuel VT, Shulman GI. Nonalcoholic Fatty Liver Disease as a Nexus of Metabolic and Hepatic Diseases.

- Cell Metab. 2018; 27:22–41.
<https://doi.org/10.1016/j.cmet.2017.08.002>
PMID:[28867301](https://pubmed.ncbi.nlm.nih.gov/28867301/)
5. Derynck R, Zhang YE. Smad-dependent and Smad-independent pathways in TGF-beta family signalling. *Nature*. 2003; 425:577–84.
<https://doi.org/10.1038/nature02006> PMID:[14534577](https://pubmed.ncbi.nlm.nih.gov/14534577/)
 6. Luu HH, Song WX, Luo X, Manning D, Luo J, Deng ZL, Sharff KA, Montag AG, Haydon RC, He TC. Distinct roles of bone morphogenetic proteins in osteogenic differentiation of mesenchymal stem cells. *J Orthop Res*. 2007; 25:665–77.
<https://doi.org/10.1002/jor.20359> PMID:[17290432](https://pubmed.ncbi.nlm.nih.gov/17290432/)
 7. Wang RN, Green J, Wang Z, Deng Y, Qiao M, Peabody M, Zhang Q, Ye J, Yan Z, Denduluri S, Idowu O, Li M, Shen C, et al. Bone Morphogenetic Protein (BMP) signaling in development and human diseases. *Genes Dis*. 2014; 1:87–105.
<https://doi.org/10.1016/j.gendis.2014.07.005>
PMID:[25401122](https://pubmed.ncbi.nlm.nih.gov/25401122/)
 8. Weiss A, Attisano L. The TGFbeta superfamily signaling pathway. *Wiley Interdiscip Rev Dev Biol*. 2013; 2:47–63.
<https://doi.org/10.1002/wdev.86> PMID:[23799630](https://pubmed.ncbi.nlm.nih.gov/23799630/)
 9. Salazar VS, Gamer LW, Rosen V. BMP signalling in skeletal development, disease and repair. *Nat Rev Endocrinol*. 2016; 12:203–21.
<https://doi.org/10.1038/nrendo.2016.12>
PMID:[26893264](https://pubmed.ncbi.nlm.nih.gov/26893264/)
 10. Mostafa S, Pakvasa M, Coalson E, Zhu A, Alverdy A, Castillo H, Fan J, Li A, Feng Y, Wu D, Bishop E, Du S, Spezia M, et al. The wonders of BMP9: from mesenchymal stem cell differentiation, angiogenesis, neurogenesis, tumorigenesis, and metabolism to regenerative medicine. *Genes Dis*. 2019; 6:201–23.
<https://doi.org/10.1016/j.gendis.2019.07.003>
 11. Kang Q, Song WX, Luo Q, Tang N, Luo J, Luo X, Chen J, Bi Y, He BC, Park JK, Jiang W, Tang Y, Huang J, et al. A comprehensive analysis of the dual roles of BMPs in regulating adipogenic and osteogenic differentiation of mesenchymal progenitor cells. *Stem Cells Dev*. 2009; 18:545–59.
<https://doi.org/10.1089/scd.2008.0130>
PMID:[18616389](https://pubmed.ncbi.nlm.nih.gov/18616389/)
 12. Luther G, Wagner ER, Zhu G, Kang Q, Luo Q, Lamplot J, Bi Y, Luo X, Luo J, Teven C, Shi Q, Kim SH, Gao JL, et al. BMP-9 induced osteogenic differentiation of mesenchymal stem cells: molecular mechanism and therapeutic potential. *Curr Gene Ther*. 2011; 11:229–40.
<https://doi.org/10.2174/156652311795684777>
PMID:[21453282](https://pubmed.ncbi.nlm.nih.gov/21453282/)
 13. Lamplot JD, Qin J, Nan G, Wang J, Liu X, Yin L, Tomal J, Li R, Shui W, Zhang H, Kim SH, Zhang W, Zhang J, et al. BMP9 signaling in stem cell differentiation and osteogenesis. *Am J Stem Cells*. 2013; 2:1–21.
PMID:[23671813](https://pubmed.ncbi.nlm.nih.gov/23671813/)
 14. Townsend KL, Suzuki R, Huang TL, Jing E, Schulz TJ, Lee K, Taniguchi CM, Espinoza DO, McDougall LE, Zhang H, He TC, Kokkotou E, Tseng YH. Bone morphogenetic protein 7 (BMP7) reverses obesity and regulates appetite through a central mTOR pathway. *FASEB J*. 2012; 26:2187–96.
<https://doi.org/10.1096/fj.11-199067> PMID:[22331196](https://pubmed.ncbi.nlm.nih.gov/22331196/)
 15. Tseng YH, Kokkotou E, Schulz TJ, Huang TL, Winnay JN, Taniguchi CM, Tran TT, Suzuki R, Espinoza DO, Yamamoto Y, Ahrens MJ, Dudley AT, Norris AW, et al. New role of bone morphogenetic protein 7 in brown adipogenesis and energy expenditure. *Nature*. 2008; 454:1000–04.
<https://doi.org/10.1038/nature07221> PMID:[18719589](https://pubmed.ncbi.nlm.nih.gov/18719589/)
 16. Qian SW, Tang Y, Li X, Liu Y, Zhang YY, Huang HY, Xue RD, Yu HY, Guo L, Gao HD, Liu Y, Sun X, Li YM, et al. BMP4-mediated brown fat-like changes in white adipose tissue alter glucose and energy homeostasis. *Proc Natl Acad Sci USA*. 2013; 110:E798–807.
<https://doi.org/10.1073/pnas.1215236110>
PMID:[23388637](https://pubmed.ncbi.nlm.nih.gov/23388637/)
 17. Modica S, Straub LG, Balaz M, Sun W, Varga L, Stefanicka P, Profant M, Simon E, Neubauer H, Ukropcova B, Ukropec J, Wolfrum C. Bmp4 Promotes a Brown to White-like Adipocyte Shift. *Cell Rep*. 2016; 16:2243–58.
<https://doi.org/10.1016/j.celrep.2016.07.048>
PMID:[27524617](https://pubmed.ncbi.nlm.nih.gov/27524617/)
 18. Elsen M, Raschke S, Tennagels N, Schwahn U, Jelenik T, Roden M, Romacho T, Eckel J. BMP4 and BMP7 induce the white-to-brown transition of primary human adipose stem cells. *Am J Physiol Cell Physiol*. 2014; 306:C431–40.
<https://doi.org/10.1152/ajpcell.00290.2013>
PMID:[24284793](https://pubmed.ncbi.nlm.nih.gov/24284793/)
 19. Hoffmann JM, Grünberg JR, Church C, Elias I, Palsdottir V, Jansson JO, Bosch F, Hammarstedt A, Hedjazifar S, Smith U. BMP4 Gene Therapy in Mature Mice Reduces BAT Activation but Protects from Obesity by Browning Subcutaneous Adipose Tissue. *Cell Rep*. 2017; 20:1038–49.
<https://doi.org/10.1016/j.celrep.2017.07.020>
PMID:[28768190](https://pubmed.ncbi.nlm.nih.gov/28768190/)
 20. Qian SW, Wu MY, Wang YN, Zhao YX, Zou Y, Pan JB, Tang Y, Liu Y, Guo L, Tang QQ. BMP4 facilitates beige fat biogenesis via regulating adipose tissue macrophages. *J Mol Cell Biol*. 2019; 11:14–25.
<https://doi.org/10.1093/jmcb/mjy011> PMID:[29462349](https://pubmed.ncbi.nlm.nih.gov/29462349/)

21. Ricchi M, Odoardi MR, Carulli L, Anzivino C, Ballestri S, Pinetti A, Fantoni LI, Marra F, Bertolotti M, Banni S, Lonardo A, Carulli N, Loria P. Differential effect of oleic and palmitic acid on lipid accumulation and apoptosis in cultured hepatocytes. *J Gastroenterol Hepatol*. 2009; 24:830–40.
<https://doi.org/10.1111/j.1440-1746.2008.05733.x>
PMID:[19207680](https://pubmed.ncbi.nlm.nih.gov/19207680/)
22. Chang JJ, Hsu MJ, Huang HP, Chung DJ, Chang YC, Wang CJ. Mulberry anthocyanins inhibit oleic acid induced lipid accumulation by reduction of lipogenesis and promotion of hepatic lipid clearance. *J Agric Food Chem*. 2013; 61:6069–76.
<https://doi.org/10.1021/jf401171k> PMID:[23731091](https://pubmed.ncbi.nlm.nih.gov/23731091/)
23. Luo J, Deng ZL, Luo X, Tang N, Song WX, Chen J, Sharff KA, Luu HH, Haydon RC, Kinzler KW, Vogelstein B, He TC. A protocol for rapid generation of recombinant adenoviruses using the AdEasy system. *Nat Protoc*. 2007; 2:1236–47.
<https://doi.org/10.1038/nprot.2007.135>
PMID:[17546019](https://pubmed.ncbi.nlm.nih.gov/17546019/)
24. He TC, Zhou S, da Costa LT, Yu J, Kinzler KW, Vogelstein B. A simplified system for generating recombinant adenoviruses. *Proc Natl Acad Sci USA*. 1998; 95:2509–14.
<https://doi.org/10.1073/pnas.95.5.2509>
PMID:[9482916](https://pubmed.ncbi.nlm.nih.gov/9482916/)
25. Wang EA, Israel DI, Kelly S, Luxenberg DP. Bone morphogenetic protein-2 causes commitment and differentiation in C3H10T1/2 and 3T3 cells. *Growth Factors*. 1993; 9:57–71.
<https://doi.org/10.3109/08977199308991582>
PMID:[8347351](https://pubmed.ncbi.nlm.nih.gov/8347351/)
26. Zamani N, Brown CW. Emerging roles for the transforming growth factor- β superfamily in regulating adiposity and energy expenditure. *Endocr Rev*. 2011; 32:387–403.
<https://doi.org/10.1210/er.2010-0018> PMID:[21173384](https://pubmed.ncbi.nlm.nih.gov/21173384/)
27. Tang QQ, Otto TC, Lane MD. Commitment of C3H10T1/2 pluripotent stem cells to the adipocyte lineage. *Proc Natl Acad Sci USA*. 2004; 101:9607–11.
<https://doi.org/10.1073/pnas.0403100101>
PMID:[15210946](https://pubmed.ncbi.nlm.nih.gov/15210946/)
28. Huang H, Song TJ, Li X, Hu L, He Q, Liu M, Lane MD, Tang QQ. BMP signaling pathway is required for commitment of C3H10T1/2 pluripotent stem cells to the adipocyte lineage. *Proc Natl Acad Sci USA*. 2009; 106:12670–75.
<https://doi.org/10.1073/pnas.0906266106>
PMID:[19620713](https://pubmed.ncbi.nlm.nih.gov/19620713/)
29. Gustafson B, Hammarstedt A, Hedjazifar S, Hoffmann JM, Svensson PA, Grimsby J, Rondinone C, Smith U. BMP4 and BMP Antagonists Regulate Human White and Beige Adipogenesis. *Diabetes*. 2015; 64:1670–81.
<https://doi.org/10.2337/db14-1127> PMID:[25605802](https://pubmed.ncbi.nlm.nih.gov/25605802/)
30. Son JW, Kim MK, Park YM, Baek KH, Yoo SJ, Song KH, Son HS, Yoon KH, Lee WC, Cha BY, Son HY, Kwon HS. Association of serum bone morphogenetic protein 4 levels with obesity and metabolic syndrome in non-diabetic individuals. *Endocr J*. 2011; 58:39–46.
<https://doi.org/10.1507/endocrj.K10E-248>
PMID:[21186333](https://pubmed.ncbi.nlm.nih.gov/21186333/)
31. Böttcher Y, Unbehauen H, Klötting N, Ruschke K, Körner A, Schleinitz D, Tönjes A, Enigk B, Wolf S, Dietrich K, Koriath M, Scholz GH, Tseng YH, et al. Adipose tissue expression and genetic variants of the bone morphogenetic protein receptor 1A gene (BMPR1A) are associated with human obesity. *Diabetes*. 2009; 58:2119–28.
<https://doi.org/10.2337/db08-1458> PMID:[19502417](https://pubmed.ncbi.nlm.nih.gov/19502417/)
32. Schleinitz D, Klötting N, Böttcher Y, Wolf S, Dietrich K, Tönjes A, Breitfeld J, Enigk B, Halbritter J, Körner A, Schön MR, Jenkner J, Tseng YH, et al. Genetic and evolutionary analyses of the human bone morphogenetic protein receptor 2 (BMPR2) in the pathophysiology of obesity. *PLoS One*. 2011; 6:e16155.
<https://doi.org/10.1371/journal.pone.0016155>
PMID:[21311592](https://pubmed.ncbi.nlm.nih.gov/21311592/)
33. Thorpe LM, Yuzugullu H, Zhao JJ. PI3K in cancer: divergent roles of isoforms, modes of activation and therapeutic targeting. *Nat Rev Cancer*. 2015; 15:7–24.
<https://doi.org/10.1038/nrc3860> PMID:[25533673](https://pubmed.ncbi.nlm.nih.gov/25533673/)
34. Fruman DA, Chiu H, Hopkins BD, Bagrodia S, Cantley LC, Abraham RT. The PI3K Pathway in Human Disease. *Cell*. 2017; 170:605–35.
<https://doi.org/10.1016/j.cell.2017.07.029>
PMID:[28802037](https://pubmed.ncbi.nlm.nih.gov/28802037/)
35. Han J, Wang Y. mTORC1 signaling in hepatic lipid metabolism. *Protein Cell*. 2018; 9:145–151.
<https://doi.org/10.1007/s13238-017-0409-3>
PMID:[28434145](https://pubmed.ncbi.nlm.nih.gov/28434145/)
36. Saxton RA, Sabatini DM. mTOR Signaling in Growth, Metabolism, and Disease. *Cell*. 2017; 168:960–76.
<https://doi.org/10.1016/j.cell.2017.02.004>
PMID:[28283069](https://pubmed.ncbi.nlm.nih.gov/28283069/)
37. Lamming DW, Sabatini DM. A Central role for mTOR in lipid homeostasis. *Cell Metab*. 2013; 18:465–69.
<https://doi.org/10.1016/j.cmet.2013.08.002>
PMID:[23973332](https://pubmed.ncbi.nlm.nih.gov/23973332/)
38. Rui L. Energy metabolism in the liver. *Compr Physiol*. 2014; 4:177–97.
<https://doi.org/10.1002/cphy.c130024>
PMID:[24692138](https://pubmed.ncbi.nlm.nih.gov/24692138/)

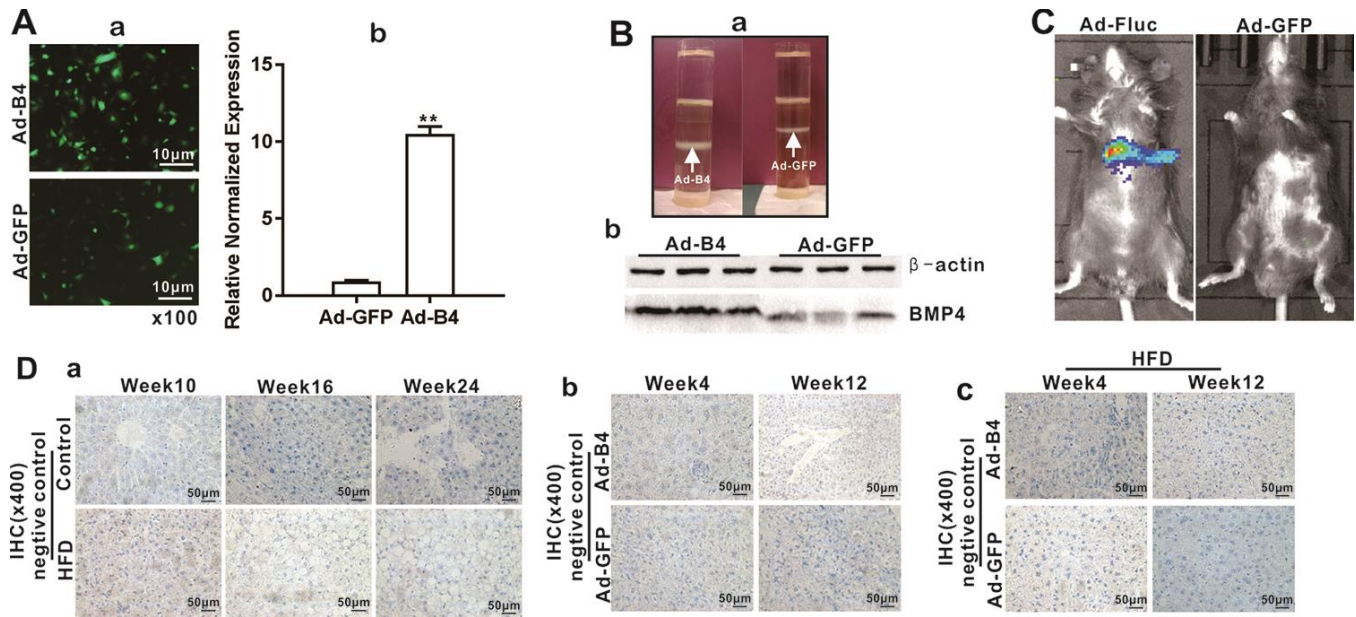
39. Wang Y, Viscarra J, Kim SJ, Sul HS. Transcriptional regulation of hepatic lipogenesis. *Nat Rev Mol Cell Biol*. 2015; 16:678–89. <https://doi.org/10.1038/nrm4074> PMID:26490400
40. Düvel K, Yecies JL, Menon S, Raman P, Lipovsky AI, Souza AL, Triantafellow E, Ma Q, Gorski R, Cleaver S, Vander Heiden MG, MacKeigan JP, Finan PM, et al. Activation of a metabolic gene regulatory network downstream of mTOR complex 1. *Mol Cell*. 2010; 39:171–83. <https://doi.org/10.1016/j.molcel.2010.06.022> PMID:20670887
41. Han J, Li E, Chen L, Zhang Y, Wei F, Liu J, Deng H, Wang Y. The CREB coactivator CRTC2 controls hepatic lipid metabolism by regulating SREBP1. *Nature*. 2015; 524:243–6. <https://doi.org/10.1038/nature14557> PMID:26147081
42. Porstmann T, Santos CR, Griffiths B, Cully M, Wu M, Leever S, Griffiths JR, Chung YL, Schulze A. SREBP activity is regulated by mTORC1 and contributes to Akt-dependent cell growth. *Cell Metab*. 2008; 8:224–36. <https://doi.org/10.1016/j.cmet.2008.07.007> PMID:18762023
43. Peterson TR, Sengupta SS, Harris TE, Carmack AE, Kang SA, Balderas E, Guertin DA, Madden KL, Carpenter AE, Finck BN, Sabatini DM. mTOR complex 1 regulates lipin 1 localization to control the SREBP pathway. *Cell*. 2011; 146:408–20. <https://doi.org/10.1016/j.cell.2011.06.034> PMID:21816276
44. Wu N, Zhang H, Deng F, Li R, Zhang W, Chen X, Wen S, Wang N, Zhang J, Yin L, Liao Z, Zhang Z, Zhang Q, et al. Overexpression of Ad5 precursor terminal protein accelerates recombinant adenovirus packaging and amplification in HEK-293 packaging cells. *Gene Ther*. 2014; 21:629–37. <https://doi.org/10.1038/gt.2014.40> PMID:24784448
45. Wei Q, Fan J, Liao J, Zou Y, Song D, Liu J, Cui J, Liu F, Ma C, Hu X, Li L, Yu Y, Qu X, et al. Engineering the Rapid Adenovirus Production and Amplification (RAPA) Cell Line to Expedite the Generation of Recombinant Adenoviruses. *Cell Physiol Biochem*. 2017; 41:2383–98. <https://doi.org/10.1159/000475909> PMID:28463838
46. Seglen PO. Preparation of isolated rat liver cells. *Methods Cell Biol*. 1976; 13:29–83. [https://doi.org/10.1016/S0091-679X\(08\)61797-5](https://doi.org/10.1016/S0091-679X(08)61797-5) PMID:177845
47. Cheng H, Jiang W, Phillips FM, Haydon RC, Peng Y, Zhou L, Luu HH, An N, Breyer B, Vanichakarn P, Szatkowski JP, Park JY, He TC. Osteogenic activity of the fourteen types of human bone morphogenetic proteins (BMPs). *J Bone Joint Surg Am*. 2003; 85:1544–52. <https://doi.org/10.2106/00004623-200308000-00017> PMID:12925636
48. Zhang L, Luo Q, Shu Y, Zeng Z, Huang B, Feng Y, Zhang B, Wang X, Lei Y, Ye Z, Zhao L, Cao D, Yang L, et al. Transcriptomic landscape regulated by the 14 types of bone morphogenetic proteins (BMPs) in lineage commitment and differentiation of mesenchymal stem cells (MSCs). *Genes Dis*. 2019; 6:258–75. <https://doi.org/10.1016/j.gendis.2019.03.008>
49. Cui J, Zhang W, Huang E, Wang J, Liao J, Li R, Yu X, Zhao C, Zeng Z, Shu Y, Zhang R, Yan S, Lei J, et al. BMP9-induced osteoblastic differentiation requires functional Notch signaling in mesenchymal stem cells. *Lab Invest*. 2019; 99:58–71. <https://doi.org/10.1038/s41374-018-0087-7> PMID:30353129
50. Wang X, Yuan C, Huang B, Fan J, Feng Y, Li AJ, Zhang B, Lei Y, Ye Z, Zhao L, Cao D, Yang L, Wu D, et al. Developing a Versatile Shotgun Cloning Strategy for Single-Vector-Based Multiplex Expression of Short Interfering RNAs (siRNAs) in Mammalian Cells. *ACS Synth Biol*. 2019; 8:2092–105. <https://doi.org/10.1021/acssynbio.9b00203> PMID:31465214
51. Yan S, Zhang R, Wu K, Cui J, Huang S, Ji X, An L, Yuan C, Gong C, Zhang L, Liu W, Feng Y, Zhang B, et al. Characterization of the essential role of bone morphogenetic protein 9 (BMP9) in osteogenic differentiation of mesenchymal stem cells (MSCs) through RNA interference. *Genes Dis*. 2018; 5:172–84. <https://doi.org/10.1016/j.gendis.2018.04.006> PMID:30258947
52. Zhao C, Wu N, Deng F, Zhang H, Wang N, Zhang W, Chen X, Wen S, Zhang J, Yin L, Liao Z, Zhang Z, Zhang Q, et al. Adenovirus-mediated gene transfer in mesenchymal stem cells can be significantly enhanced by the cationic polymer polybrene. *PLoS One*. 2014; 9:e92908. <https://doi.org/10.1371/journal.pone.0092908> PMID:24658746
53. Kang Q, Sun MH, Cheng H, Peng Y, Montag AG, Deyrup AT, Jiang W, Luu HH, Luo J, Szatkowski JP, Vanichakarn P, Park JY, Li Y, et al. Characterization of the distinct orthotopic bone-forming activity of 14 BMPs using recombinant adenovirus-mediated gene delivery. *Gene Ther*. 2004; 11:1312–20. <https://doi.org/10.1038/sj.gt.3302298> PMID:15269709
54. Huang E, Bi Y, Jiang W, Luo X, Yang K, Gao JL, Gao Y, Luo Q, Shi Q, Kim SH, Liu X, Li M, Hu N, et al. Conditionally immortalized mouse embryonic fibroblasts retain proliferative activity without

- compromising multipotent differentiation potential. *PLoS One*. 2012; 7:e32428.
<https://doi.org/10.1371/journal.pone.0032428>
PMID:[22384246](https://pubmed.ncbi.nlm.nih.gov/22384246/)
55. Fan J, Feng Y, Zhang R, Zhang W, Shu Y, Zeng Z, Huang S, Zhang L, Huang B, Wu D, Zhang B, Wang X, Lei Y, et al. A simplified system for the effective expression and delivery of functional mature microRNAs in mammalian cells. *Cancer Gene Ther*. 2019. [Epub ahead of print].
<https://doi.org/10.1038/s41417-019-0113-y>
PMID:[31222181](https://pubmed.ncbi.nlm.nih.gov/31222181/)
56. Zhu Y, Shi Q, Peng Q, Gao Y, Yang T, Cheng Y, Wang H, Luo Y, Huang A, He TC, Fan J. A simplified 3D liver microsphere tissue culture model for hepatic cell signaling and drug-induced hepatotoxicity studies. *Int J Mol Med*. 2019; 44:1653–1666.
<https://doi.org/10.3892/ijmm.2019.4321>
PMID:[31485603](https://pubmed.ncbi.nlm.nih.gov/31485603/)
57. Deng Y, Wang Z, Zhang F, Qiao M, Yan Z, Wei Q, Wang J, Liu H, Fan J, Zou Y, Liao J, Hu X, Chen L, et al. A Blockade of IGF Signaling Sensitizes Human Ovarian Cancer Cells to the Anthelmintic Niclosamide-Induced Anti-Proliferative and Anticancer Activities. *Cell Physiol Biochem*. 2016; 39:871–88.
<https://doi.org/10.1159/000447797> PMID:[27497986](https://pubmed.ncbi.nlm.nih.gov/27497986/)
58. Fan J, Wei Q, Liao J, Zou Y, Song D, Xiong D, Ma C, Hu X, Qu X, Chen L, Li L, Yu Y, Yu X, et al. Noncanonical Wnt signaling plays an important role in modulating canonical Wnt-regulated stemness, proliferation and terminal differentiation of hepatic progenitors. *Oncotarget*. 2017; 8:27105–19.
<https://doi.org/10.18632/oncotarget.15637>
PMID:[28404920](https://pubmed.ncbi.nlm.nih.gov/28404920/)
59. Livak KJ, Schmittgen TD. Analysis of relative gene expression data using real-time quantitative PCR and the 2⁻(-Delta Delta C(T)) Method. *Methods*. 2001; 25:402–08.
<https://doi.org/10.1006/meth.2001.1262>
PMID:[11846609](https://pubmed.ncbi.nlm.nih.gov/11846609/)
60. Zhou L, An N, Jiang W, Haydon R, Cheng H, Zhou Q, Breyer B, Feng T, He TC. Fluorescence-based functional assay for Wnt/beta-catenin signaling activity. *Biotechniques*. 2002; 33:1126–8, 1130, 1132.
<https://doi.org/10.2144/02335ddd07>
PMID:[12449394](https://pubmed.ncbi.nlm.nih.gov/12449394/)
61. Huang B, Huang LF, Zhao L, Zeng Z, Wang X, Cao D, Yang L, Ye Z, Chen X, Liu B, He TC, Wang X. Microvesicles (MIVs) secreted from adipose-derived stem cells (ADSCs) contain multiple microRNAs and promote the migration and invasion of endothelial cells. *Genes Dis*. 2019. [Epub ahead of print].
<https://doi.org/10.1016/j.gendis.2019.04.005>
62. Parasuraman S, Raveendran R, Kesavan R. Blood sample collection in small laboratory animals. *J Pharmacol Pharmacother*. 2010; 1:87–93.
<https://doi.org/10.4103/0976-500X.72350>
PMID:[21350616](https://pubmed.ncbi.nlm.nih.gov/21350616/)
63. National Research Council (US) Committee for the Update of the Guide for the Care and Use of Laboratory Animals. *Guide for the Care and Use of Laboratory Animals*. 8th edition. Washington (DC): National Academies Press (US); 2011.
<https://doi.org/10.17226/12910> PMID:[21595115](https://pubmed.ncbi.nlm.nih.gov/21595115/)
64. Wu J, Wang C, Li S, Li S, Wang W, Li J, Chi Y, Yang H, Kong X, Zhou Y, Dong C, Wang F, Xu G, et al. Thyroid hormone-responsive SPOT 14 homolog promotes hepatic lipogenesis, and its expression is regulated by liver X receptor α through a sterol regulatory element-binding protein 1c-dependent mechanism in mice. *Hepatology*. 2013; 58:617–28.
<https://doi.org/10.1002/hep.26272> PMID:[23348573](https://pubmed.ncbi.nlm.nih.gov/23348573/)
65. Huang X, Wang F, Zhao C, Yang S, Cheng Q, Tang Y, Zhang F, Zhang Y, Luo W, Wang C, Zhou P, Kim S, Zuo G, et al. Dentinogenesis and Tooth-Alveolar Bone Complex Defects in *BMP9/GDF2* Knockout Mice. *Stem Cells Dev*. 2019; 28:683–94.
<https://doi.org/10.1089/scd.2018.0230>
PMID:[30816068](https://pubmed.ncbi.nlm.nih.gov/30816068/)
66. Zhao C, Qazvini NT, Sadati M, Zeng Z, Huang S, De La Lastra AL, Zhang L, Feng Y, Liu W, Huang B, Zhang B, Dai Z, Shen Y, et al. A pH-Triggered, Self-Assembled, and Bioprintable Hybrid Hydrogel Scaffold for Mesenchymal Stem Cell Based Bone Tissue Engineering. *ACS Appl Mater Interfaces*. 2019; 11:8749–62.
<https://doi.org/10.1021/acsami.8b19094>
PMID:[30734555](https://pubmed.ncbi.nlm.nih.gov/30734555/)
67. Yu X, Chen L, Wu K, Yan S, Zhang R, Zhao C, Zeng Z, Shu Y, Huang S, Lei J, Ji X, Yuan C, Zhang L, et al. Establishment and functional characterization of the reversibly immortalized mouse glomerular podocytes (imPODs). *Genes Dis*. 2018; 5:137–49.
<https://doi.org/10.1016/j.gendis.2018.04.003>
PMID:[30258943](https://pubmed.ncbi.nlm.nih.gov/30258943/)
68. Yu X, Liu F, Zeng L, He F, Zhang R, Yan S, Zeng Z, Shu Y, Zhao C, Wu X, Lei J, Zhang W, Yang C, et al. Niclosamide Exhibits Potent Anticancer Activity and Synergizes with Sorafenib in Human Renal Cell Cancer Cells. *Cell Physiol Biochem*. 2018; 47:957–71.
<https://doi.org/10.1159/000490140>
PMID:[29843133](https://pubmed.ncbi.nlm.nih.gov/29843133/)
69. Wang X, Wu X, Zhang Z, Ma C, Wu T, Tang S, Zeng Z, Huang S, Gong C, Yuan C, Zhang L, Feng Y, Huang B, et

- al. Monensin inhibits cell proliferation and tumor growth of chemo-resistant pancreatic cancer cells by targeting the EGFR signaling pathway. *Sci Rep.* 2018; 8:17914.
<https://doi.org/10.1038/s41598-018-36214-5>
PMID:[30559409](https://pubmed.ncbi.nlm.nih.gov/30559409/)
70. Liao Z, Nan G, Yan Z, Zeng L, Deng Y, Ye J, Zhang Z, Qiao M, Li R, Denduluri S, Wang J, Wei Q, Geng N, et al. The Anthelmintic Drug Niclosamide Inhibits the Proliferative Activity of Human Osteosarcoma Cells by Targeting Multiple Signal Pathways. *Curr Cancer Drug Targets.* 2015; 15:726–38.
<https://doi.org/10.2174/1568009615666150629132157>
PMID:[26118906](https://pubmed.ncbi.nlm.nih.gov/26118906/)
71. Crettaz J, Berraondo P, Mauleón I, Ochoa-Callejero L, Shankar V, Barajas M, van Rooijen N, Kochanek S, Qian C, Prieto J, Hernández-Alcoceba R, González-Aseguinolaza G. Intrahepatic injection of adenovirus reduces inflammation and increases gene transfer and therapeutic effect in mice. *Hepatology.* 2006; 44:623–32.
<https://doi.org/10.1002/hep.21292>
PMID:[16941711](https://pubmed.ncbi.nlm.nih.gov/16941711/)

SUPPLEMENTARY MATERIALS

Supplementary Figure



Supplementary Figure 1. (A) Ad-BMP4-mediated transgene expression in mouse hepatocytes. Ad-B4 or Ad-GFP were used to infect mouse primary hepatocytes isolated from 4-week-old mice for 48h. Total RNA was isolated for TqPCR analysis of the expression of human BMP4. Relative expression was calculated by dividing the relative expression values (i.e., *gene/Gapdh*) in “***” $p < 0.01$, Ad-B4 group vs. Ad-GFP group. (B) Ad-B4-mediated transgene expression post intrahepatic injections. High titer recombinant adenoviruses Ad-B4 and Ad-GFP were purified via CsCl gradient ultracentrifugation (a). The desired virus bands are indicated by arrows. The 4-week-old mice were subjected to the intrahepatic injection of Ad-B4 or Ad-GFP (10^{10} pfu in 30µl PBS/injection/animal, n=3 each virus) and sacrificed after 5 days. The retrieved liver samples were subjected to Western blotting to detect BMP4 expression(b). (C) Adenovirus-mediated transgene expression lasts more than 5 days post intrahepatic injection. The CsCl gradient purified Ad-Fluc and Ad-GFP were intrahepatically injected into 4-week-old mice. The mice were subjected to optical bioluminescence imaging with a luciferin substrate at different time points after adenovirus administration. Representative imaging results at day 5 of intrahepatic injection are shown. (D) Paraffin sections of liver samples were subjected to IHC staining, stains without primary antibody were used as negative controls. The liver samples prepared in Figure 1 (a), The liver samples prepared in Figure 4 (b), The liver samples prepared in Figure 4 (c).

Supplementary Tables

Supplemental Table 1. List of TqPCR Primers.

Gene	Forward primer	Reverse primer	Accession No.
<i>mouse Gapdh</i>	ACCCAGAAGACTGTGGATGG	CACATTGGGGGTAGGAACAC	NM_008084
<i>mouse Bmp4</i>	GCGAGCCATGCTAGTTTGA	AAGTGTGCCTCGAAGTCC	NM_001316360.1
<i>human BMP4</i>	GGGAAAGGGGCTTCCACC	TTTGGCTGCTTCTCCCGG	NM_001202.5
<i>mouse Gpam</i>	TTCCTGCACGCCACAGAG	TCTCGCCAGCCATCCTCT	NM_001356285.1
<i>mouse Mogat1</i>	CCTTCCTCCTGCTCGTGC	GCCAGCTTTGGACCCAGT	NM_026713.3
<i>mouse Fasn</i>	CTCGGCTCGATGGCTCAG	GGGATGTGCCACAGTGCT	NM_007988.3
<i>mouse Acaca</i>	GTGTTTGCTGGCCAGTGC	TGCCCCTGTGAAGCTCAG	NM_133360.2
<i>mouse Apoc3</i>	ACCCAGCCATCTAGCCCA	ACAGAGCCCAGCAGCAAG	NM_001289755.1
<i>mouse Srebfl/Srebp</i>	GACCCTACGAAGTGCACACA	GTGGCCTAGTCACAGGTTCC	NM_001313979.1
<i>mouse Plin2</i>	GAACCAGCCAACGTCCGA	TCCTTTCCACGCTGCCAG	NM_007408.3
<i>mouse Plin3</i>	GAGCATGTGTGTGGCCCT	CTCTGGCTATGCGCTCCC	NM_025836.3
<i>mouse Scd1</i>	TGCCGCGCATCTCTATGG	AGTTGTGGAAGCCCTCGC	NM_009127.4
<i>mouse Lipe</i>	CGTGCCAGCCACAACCTA	TGCAGGAAGTCAGCGGTG	NM_001039507.2
<i>mouse Ctnnb1</i>	TGCAGCTTCTGGGTTCCG	GCACAGATGGCAGGCTCA	NM_001165902.1
<i>mouse Ascl1</i>	GGAAGCAGGATGGCAGCA	GCCCCTGTAGGTTGGCTG	NM_008553.4
<i>mouse Acat2</i>	GCATGACAGCCACCACCT	GCTGTCCACCTGGGTTCC	NM_009338.3
<i>mouse Cpt1b</i>	GGAGGTGGCTTTGGTCCC	GGCGGATGTGGTTCCCAA	NM_009948.2
<i>mouse Ndufs4</i>	GGCGAAGGGCAATGGCTA	GCTGTGTGTCCCGAGTCT	NM_010887.2
<i>mouse Pck2</i>	GCTTACGTGGTGGCCAGT	CACGTGGCCAATCAGGGT	NM_028994.2
<i>mouse Cyp1a2</i>	CCAGTCAGCCAGGTGGTG	CTCTTGAGGGCCGGGTTG	NM_009993
<i>mouse Acads(Bcl-1)</i>	CACGCTGGGCAAGAAGGA	TGCCAATGCGACCCATGT	NM_007383.3
<i>mouse Acadm</i>	CGGAGGCAGCAGATCGAG	CTTGCGGGCAGTTGCTTG	NM_007382.5
<i>mouse Atp5a1</i>	GCACGGGCTGAGGAATGT	CCAACAGCTCCTCGCAA	NM_007505.2
<i>mouse Hadha</i>	ACCACAGGCTTCGGCTTC	GCGACCAAGAAGCCCTT	NM_130826.2
<i>mouse Deptor</i>	GTCAGCCCCAGCAAGGAG	TGGGGTTGCAGAGCACAG	NM_001037937.3
<i>mouse Pras40/Akt1s1</i>	GGCCAGGGAGGATGAGGA	TGTGCTCTCCGGGTCTGA	NM_001253920.1
<i>mouse Rptor</i>	ACGTGCGCATTGTCAGGA	CGGATCGAGCCATCACCC	NM_001306081.1
<i>mouse Mtor</i>	AAGGACCTCACGCAAGCC	ATTGGCTGGTTGGGGTCG	NM_020009.2
<i>mouse Lipin1</i>	AACGGAGCCGACACCTTG	GCTCCGTTGTCAGTGGCT	NM_001130412.1
<i>mouse Rps6kb1/S6k</i>	CCTAGCGCCTGACTTCCG	CCCCCTCCTCCAGCTCAT	NM_001114334.2

Supplemental Table 2. Formula and fatty acid composition of control (10% fat) and high fat (45% fat) diets.

	MD10% Fat	MD45% Fat
Energy Composition	100	100
Protein	20	20
Carbohydrate	70	35
Fat	10	45
Composition of fatty acid	100	100
Saturated (%)	28.7	40.3
Monounsaturated (%)	32.7	40.4
Polyunsaturated (%)	38.6	19.3
Type of fat (gm)	45	202.5
Lard	20	177.5
Soybean Oil	25	25
Fatty acid profile (gm)	42.2	190.6
C2, Acetic	0	0
C4, Butyric	0	0
C6, Caproic	0	0
C8, Caprylic	0	0
C10,Capric	0.0	0.1
C12,Lauric	0.0	0.1
C14,Myristic	0.3	2.1
C15	0.0	0.2
C16,Palmitic	7.9	47.1
C16:1,Palmitoleic	0.4	3.4
C16:2	0	0
C16:3	0	0
C16:4	0	0
C17	0.1	0.6
C17:1	0	0
C18,Stearic	3.8	26.5
C18:1,Oleic	13.4	73.5
C18:2,Linoleic	14.6	32.4
C18:3,Linolenic	1.4	2.1
C18:4, Stearidonic	0	0
C20,Arachidic	0.0	0.2
C20:1	0.0	0.1
C20:2	0.1	0.4
C20:3	0.0	1.1
C20:4,Arachidonic	0.1	0.7
C20:5, Eicosapentaenoic	0	0
C21:5	0	0
C22, Behenic	0	0
C22:1, Erucic	0	0
C22:4, Clupanodonic	0	0
C22:5,Docosapentaenoic	0.0	0.2
C22:6, Docosahexaenoic	0	0
C24, Lignoceric	0	0
C24:1	0	0